

.....  
**Antimicrobial Two-Dimensional Covalent Organic Nanosheets (2D-CONs) for Fast and Highly Efficient Capture and Recovery of Phosphate Ions from Water**

Subhasis Dey, <sup>†a</sup> Sribash Das, <sup>†a</sup> Anjali Patel, <sup>†b</sup> K. Vipin Raj, <sup>c</sup> Kumar Vanka, <sup>c</sup> Debasis Manna<sup>\*ab</sup>

<sup>a</sup>Department of Chemistry, Indian Institute of Technology Guwahati, Guwahati, Assam, PIN-781039, India

<sup>b</sup>Centre for the Environment, Indian Institute of Technology Guwahati, Guwahati, Assam, PIN-781039, India

<sup>c</sup>Physical and Materials Chemistry Division, CSIR-National Chemical Laboratory (CSIR-NCL), Dr. Homi Bhabha Road, Pashan, Pune 411008, India

**Table of Contents**

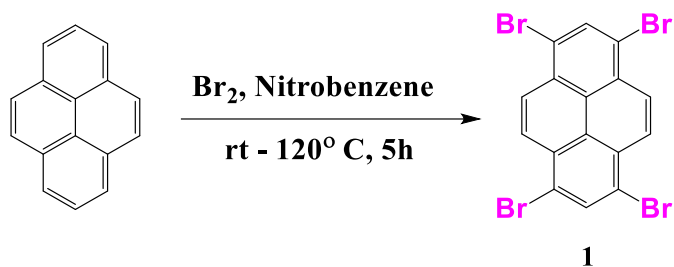
Sl. No.	Description	Page No.
1	General information	S2
2	Synthesis and characterization of the compounds	S2-10
3	Details of the DFT calculations	S10-29
4	Phosphate Adsorption analysis	S30-43
5	Antibacterial activities of the polymer	S43-46
6	<sup>1</sup> H NMR and <sup>13</sup> C NMR spectra of synthesized compounds	S47-49
7	Mass spectra of compounds	S50-51
7	References	S52-53

## 1. General information:

All reagents were purchased from Sigma-Aldrich, Merck, and other commercial sources and used directly without further purification. The column chromatography was performed using 60–120 mesh silica gels. Reactions were monitored by thin-layer chromatography (TLC) on silica gel 60 F254 (0.25 mm). The  $^1\text{H}$  NMR and  $^{13}\text{C}$  NMR were recorded at 600 and 151 MHz with Varian AS400 spectrometer and Bruker spectrometer. The chemical shifts were reported in parts per million ( $\delta$ ) using  $\text{DMSO-}d_6$  as internal solvents. The coupling constants (J values) and chemical shifts ( $\delta_{\text{ppm}}$ ) were reported in Hertz (Hz) and parts per million (ppm), respectively downfield from tetramethylsilane using residual chloroform ( $d = 7.28$  ppm for  $^1\text{H}$  NMR,  $d = 77.23$  ppm for  $^{13}\text{C}$  NMR) as an internal standard. Multiplicities are reported as follows: s (singlet), d (doublet), t (triplet), m (multiplet), and br (broadened). High-resolution mass spectra (HRMS) were recorded at Agilent Q-TOF mass spectrometer with Z-spray source using built-in software for analysis of the recorded data. Powder X-ray diffraction (PXRD) patterns were recorded on Phillips PAN analytical diffractometer for Cu  $K\alpha$  radiation ( $\alpha = 1.5406 \text{ \AA}$ ), with a scan speed of  $1^\circ \text{ min}^{-1}$  and a step size of  $0.02^\circ$  in  $2\theta$  and Rigaku MicroMax 007HF diffractometer respectively. Fourier transform infrared (FT-IR) spectra were recorded on a Bruker Optics ALPHA-E spectrometer with a universal Zn-Se ATR (attenuated total reflection) accessory in the  $600\text{--}4000 \text{ cm}^{-1}$ . Thermogravimetric analyses (TGA) were carried out on a TG50 analyzer (Mettler-Toledo) under the  $\text{N}_2$  atmosphere with a heating rate of  $10^\circ \text{C min}^{-1}$ . BET surface of the samples was measured using the Quantochrome Autosorb instrument. Before surface area analysis, the samples were activated at  $150^\circ \text{C}$  for 8 h. MALDI-TOF MS spectrum was recorded on AB SCIEX MALDI TOF/TOF<sup>TM</sup> 5800. The FETEM images were collected using a JEOL JEM 2100 transmission electron microscope (operated at a maximum accelerating voltage of 200 kV). The scanning electron microscope images were obtained using Zeiss Sigma 300 instrument operating at 10, 15, and 20 kV. X-ray photoelectron spectroscopy (XPS) analyses were performed on a Thermo Fisher Scientific Instruments UK, Sr.No.-KAS2020 with an Aluminium  $K\alpha^+$ .

## 2. Synthesis and characterization of the compounds:

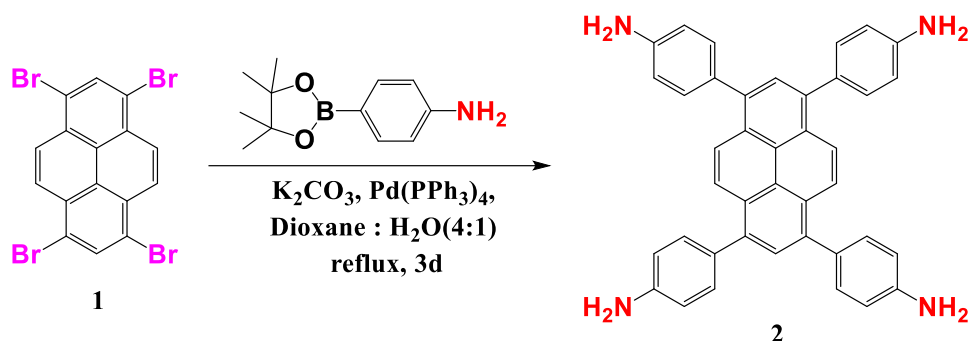
**2.1. Synthesis of 1,3,6,8-tetrabromopyrene (1)<sup>1</sup>** — To the stirring solution of pyrene (1.5 g, 7.4 mmol) in nitrobenzene (20 mL) was added (dropwise) bromine (5.23 g, 32.6 mmol) at room temperature, and the reaction mixture was stirred for 5 h at  $120^\circ \text{C}$ . After that, the reaction mixture was allowed to cool down to room temperature and filtered. The residue was washed with methanol and acetone, and excess solvent was removed under reduced pressure to obtain



**Scheme S1.** Synthesis of 1,3,6,8-tetrabromopyrene from pyrene.

1,3,6,8-tetrabromopyrene as a beige yellow solid (3.69 g, yield: 96%). The melting point of the compound is in accordance with the literature report.<sup>1</sup> The compound was used for the following reaction step without further purification.

**2.2. Synthesis of 1,3,6,8-tetrakis(4-aminophenyl)pyrene (Py(NH<sub>2</sub>)<sub>4</sub>)<sup>2</sup>** — To a stirring solution of 1,4-dioxane (32 mL) and degassed H<sub>2</sub>O (8 mL) were sequentially added 1,3,6,8-tetrabromopyrene (1.482 g, 2.86 mmol), 4-aminophenylboronic acid pinacol ester (3.01 g, 13.7 mmol), K<sub>2</sub>CO<sub>3</sub> (2.175 g, 15.7 mmol) and Pd(PPh<sub>3</sub>)<sub>4</sub> (300 mg, 0.29 mmol, 10 mol%) and the

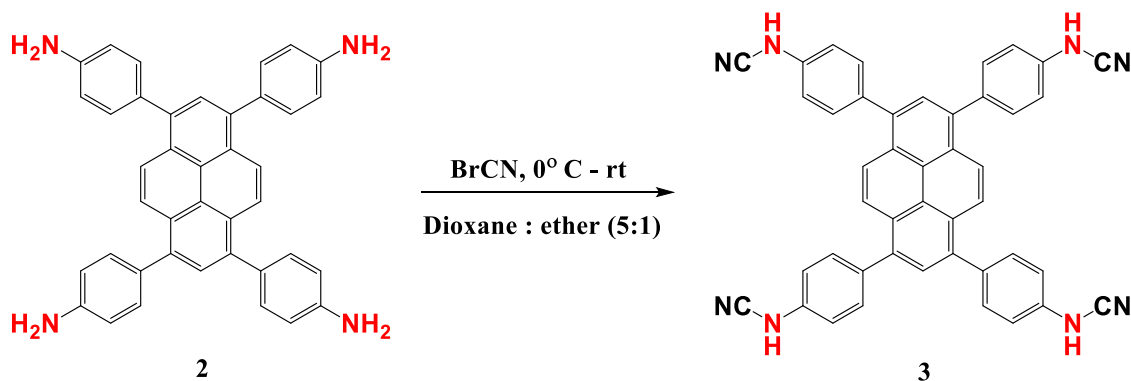


**Scheme S2.** Synthesis of 1,3,6,8-tetrakis(4-aminophenyl)pyrene (Py(NH<sub>2</sub>)<sub>4</sub>) from 1,3,6,8-tetrabromopyrene.

reaction mixture was stirred at 110° C for 3 days. The reaction mixture was cooled down to room temperature, and H<sub>2</sub>O was added to quench the reaction. The obtained precipitate was filtered and sequentially washed with H<sub>2</sub>O (100 mL), methanol (80 mL), and diethyl ether (50 mL). The obtained solid was further purified by recrystallization from chloroform/acetone to afford the target product as a greenish yellow powder (1792 mg, yield: 90%).

**Characterization of the compound:** <sup>1</sup>H NMR (600 MHz, DMSO-*d*<sub>6</sub>) δ<sub>ppm</sub> 8.20 – 8.13 (m, 4H), 7.82 – 7.79 (m, 2H), 7.43 – 7.34 (s, 8H), 6.78 – 6.69 (m, 8H), 5.42 – 5.33 (m, 8H); <sup>13</sup>C NMR (151 MHz, DMSO-*d*<sub>6</sub>) δ<sub>ppm</sub> 148.6, 137.5, 131.5, 129.4, 128.0, 127.1, 126.5, 124.8, 114.4. HRMS (ESI) calcd. for C<sub>40</sub>H<sub>30</sub>N<sub>4</sub> [M + H]<sup>+</sup>: 567.2543, found: 567.2544.<sup>2</sup>

**2.3. Synthesis of  $N,N',N'',N'''$ -(pyrene-1,3,6,8-tetrayltetrakis(benzene-4,1-diyl))tetracyanamide (3)** — To the stirring solution of compound **2** (1 g, 1.76 mmol) in 1,4-dioxane and was dropwise added cyanogen bromide (BrCN; 0.379 mL, 7.23 mmol) at 0° C.

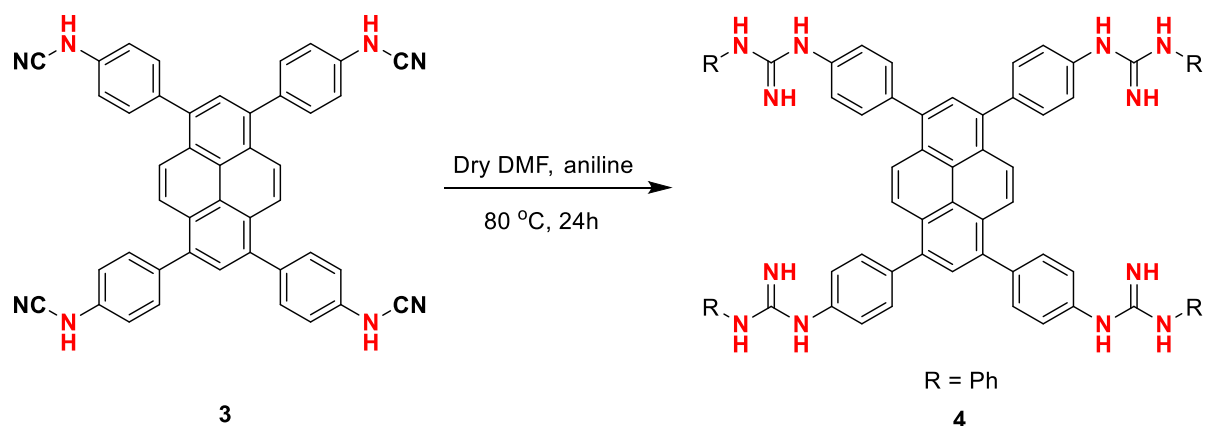


**Scheme S3.** Synthesis of  $N,N',N'',N'''$ -(pyrene-1,3,6,8-tetrayltetrakis(benzene-4,1-diyl))tetracyanamide from  $\text{Py}(\text{NH}_2)_4$ ).

The resulting reaction mixture was then stirred for 12 h at room temperature. The obtained precipitate was filtered and washed with water and 1,4-dioxane and diethyl ether. The obtained solid was further purified by recrystallization from dioxane/acetone to afford the target product as a brownish yellow powder (995 mg, 84%). **Characterisation of the compound:**  $^1\text{H}$  NMR (600 MHz,  $\text{DMSO-}d_6$ )  $\delta_{\text{ppm}}$  8.26(s, 4H), 7.92 (s, 2H), 7.50 – 7.48 (m, 4H), 7.48 – 7.47 (m, 4H), 7.18 – 7.16 (t,  $J = 6\text{Hz}$ , 4H), 7.11 – 7.09 (m, 4H), 6.92 – 6.91 (m, 4H);  $^{13}\text{C}$  NMR (151 MHz,  $\text{DMSO-}d_6$ )  $\delta_{\text{ppm}}$  139.1, 131.0, 130.1, 127.7, 126.6, 125.4, 124.2, 122.9, 115.4, 112.6. ESI-MS calcd. for  $\text{C}_{44}\text{H}_{26}\text{N}_9$   $[\text{M} + \text{NH}_4]^+$  : 684.2619, found: 684.2032.

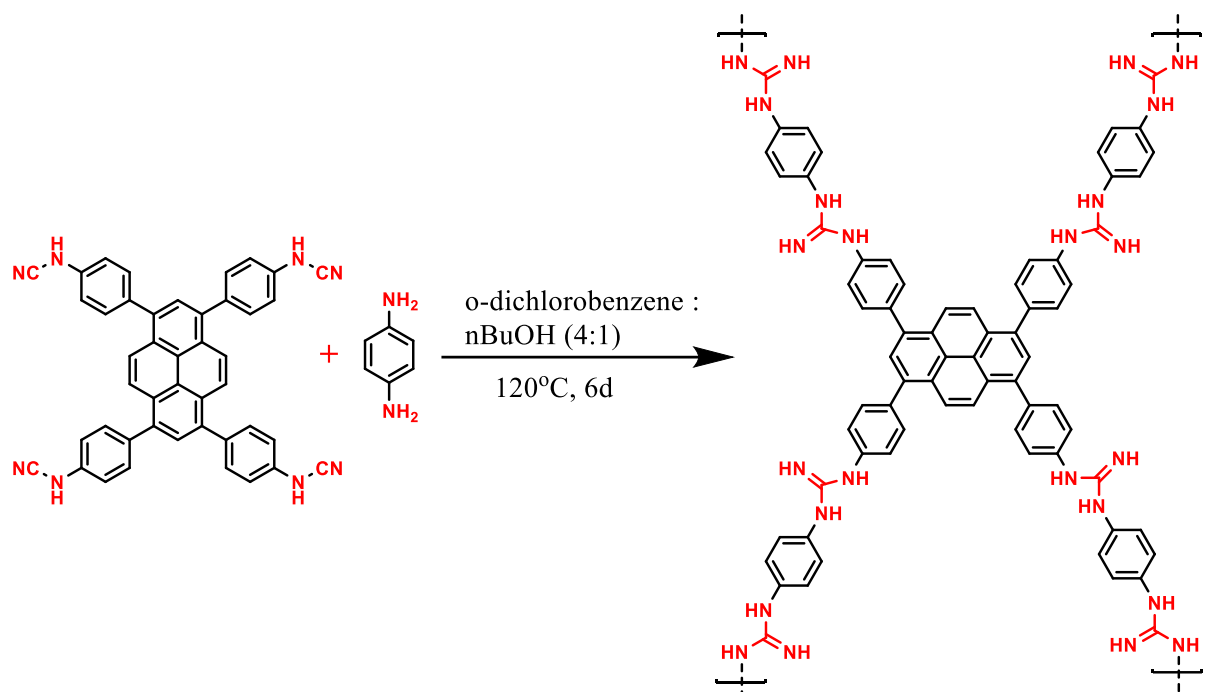
**2.4. Synthesis of  $1,1',1'',1'''$ -(pyrene-1,3,6,8-tetrayltetrakis(benzene-4,1-diyl))tetrakis(3-phenylguanidine) (4)** — **Synthesis of  $1,1',1'',1'''$ -(pyrene-1,3,6,8-tetrayltetrakis(benzene-4,1-diyl))tetrakis(3-phenylguanidine) (4)** — To the stirring solution of compound **3** (100 mg, 0.150 mmol) in dry DMF solvent in a Pyrex tube was added aniline (57 mg, 0.63 mmol) and the mixture was stirred at 80° C for 24 h. After that a dark yellow precipitate upon methanol (20 mL) addition. The precipitate was filtered and, washed with methanol followed by acetone to afford as a dark yellow solid with 83 % yield. **Characterisation of the compound:**  $^1\text{H}$  NMR (600 MHz,  $\text{DMSO-}d_6$ )  $\delta_{\text{ppm}}$  10.17 (brs, 4H), 10.12 (brs, 4H), 9.91 (brs, 4H), 8.22 – 8.18 (m, 4H), 7.97 (m, 2H), 7.74 – 7.68 (m, 16H), 7.57 – 7.52 (m, 8H), 7.42 – 7.36 (m, 4H), 7.20 – 7.07 (m, 4H), 6.84 – 6.70 (m, 4H);  $^{13}\text{C}$  NMR (151 MHz,  $\text{DMSO-}d_6$ )  $\delta_{\text{ppm}}$  154.4, 137.9, 136.7, 136.2,

131.9, 129.2, 127.9, 126.7, 124.6, 118.3, 115.7; MALDI-TOF-MS:  $C_{68}H_{54}N_{12}$  calculated for  $[M + H]^+$  1040.272, found: 1040.041.



**Scheme S4.** Synthesis of 1,1',1'',1'''-(pyrene-1,3,6,8-tetrayltetrakis(benzene-4,1-diyl))tetrakis(3-phenylguanidine) from compound **3**.

**2.5. Synthesis of gCON** — Compound **3** (0.749 mmol, 500 mg), *p*-phenylenediamine (0.898 mmol, 97.2 mg), and a solvent mixture of *o*-dichlorobenzene and *n*-BuOH (0.5 mL/0.5 mL) were taken in a Pyrex tube and was degassed by three freeze-pump-thaw cycles. The tube was sealed off and heated at 120 °C for 3 days. The precipitate was collected by centrifugation and



**Scheme S5.** Synthesis of gCON from *N,N',N'',N'''*-(pyrene-1,3,6,8-tetrayltetrakis(benzene-4,1-diyl))tetracyanamide (**3**).

washed with THF and DCM five times, subsequently washed with aqueous sodium bicarbonate ( $\text{NaHCO}_3$ ) solution. The powder was dried at  $120^\circ\text{C}$  under vacuum overnight to provide gCON with an isolated yield of 74%. **Characterisation of the compound:** IR (KBr,  $\text{cm}^{-1}$ )  $\nu = 516$  (m), 753 (s), 831 (s), 1178 (w), 1269 (s), 1508 (s), 1613 (br), 3027 (w), 3202 (w), 3326 (w).

**2.6. Chemical stability for gCON polymers** — Chemical susceptibility of gCON in common organic solvent and the acidic solution was observed. The polymer was dissolved in the solvent (THF, MeOH, Acetone, and 3N HCl) and kept at room temperature for 10 days. The chemical integrity was checked by FT-IR analysis.

**2.7. Powder X-ray Diffraction (PXRD) analysis** — The PXRD of gCON was recorded using Phillips PAN analytical diffractometer for Cu  $K\alpha$  radiation ( $\alpha = 1.5406 \text{ \AA}$ , 40 kV, 40 mA), with a scan speed of  $1^\circ \text{ min}^{-1}$  and a step size of  $0.02^\circ$  in  $2\theta$  and Rigaku MicroMax 007HF diffractometer, respectively at room temperature. This PXRD analysis showed that the nanosheet is completely amorphous in nature.

**2.8. Thermogravimetric analysis (TGA)** — The thermal stability of the gCON nanosheets was measured by TGA analysis. The experiment was carried out on a Mettler-Toledo TG50 and SDT Q600 TG-DTA analyzer under  $\text{N}_2$  atmosphere from  $20^\circ\text{C}$  to  $800^\circ\text{C}$  along with a ramp rate of  $10^\circ\text{C min}^{-1}$ .

**2.9. Transmission Electron Microscopy (TEM)** — The samples for TEM were prepared by the drop-cast method by dispersing gCON (before and after phosphate adsorption) in deionized water on a carbon-coated Cu-grid and allowed to dry overnight at  $60^\circ\text{C}$ .

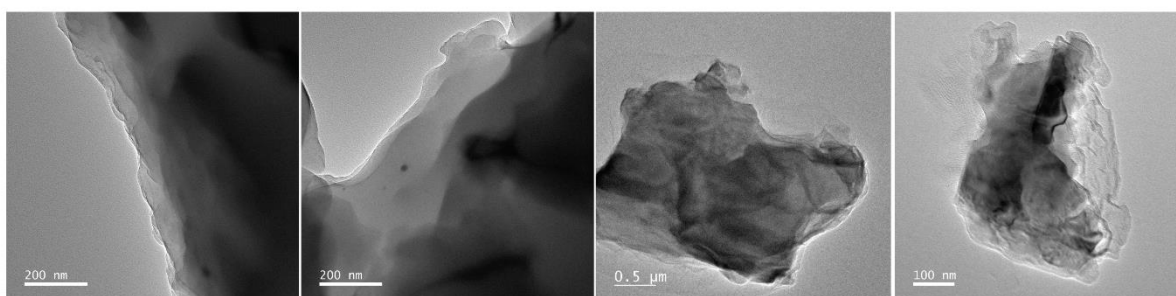


**Fig. S1.** Representative TEM images (additional) of gCONs demonstrating the presence of layered sheets.

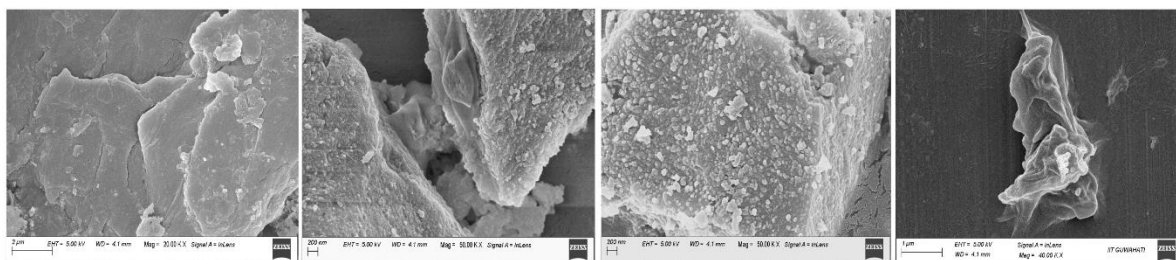


**Fig. S2.** Representative FESEM image (additional) of gCONs.

**2.10. Atomic Force Microscopy (AFM)** — The AFM images were recorded to determine the thickness and surface morphology of the COF thin films. The samples were imaged by Asylum AFM AC 240 TS-R3 silicon cantilever probes. Topographic images, amplitude, and phase images of the samples were obtained and analyzed by standard AC mode imaging. Force curves and mapping were taken by force measurement for nanomechanical mapping measurement. The nanomechanical measurements were calculated using the Hertz model.

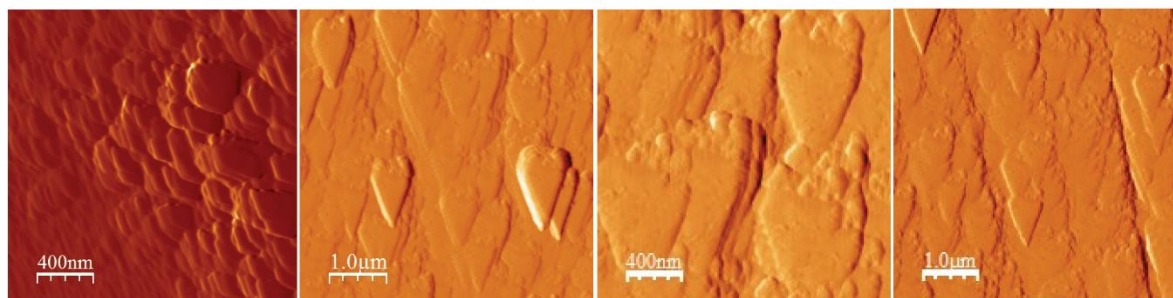


**Fig. S3.** Representative AFM image (additional) of gCONs.

**2.11. Nitrogen adsorption BET experiments** — The BET adsorption experiment was performed using Quantachrome Quadrasorb automatic and Autosorb IQ instrument. The nitrogen adsorption isotherms were collected at 77 K using a liquid nitrogen bath. Prior to the surface area analysis, the samples gCON was activated at 140 °C for 24 hours under vacuum. The porosity of BIP was measured by N<sub>2</sub> adsorption of an activated sample at 77 K. The average pore diameter of BIP was calculated by nonlocal density functional theory (NLDFT). The Brunauer-Emmet-Teller (BET) surface area of BIP was determined by Multipoint BET analysis. P and P<sub>0</sub> are the equilibrium and the saturation pressure of N<sub>2</sub>.

**2.12. X-ray photoelectron spectroscopy (XPS)** — The samples for XPS were prepared by drop-casting method dispersing gCON (before and after phosphate adsorption) in deionized

water on a silicon substrate (cleaned with isopropanol) and dried under Ar atmosphere in a desiccator.<sup>3-5</sup>

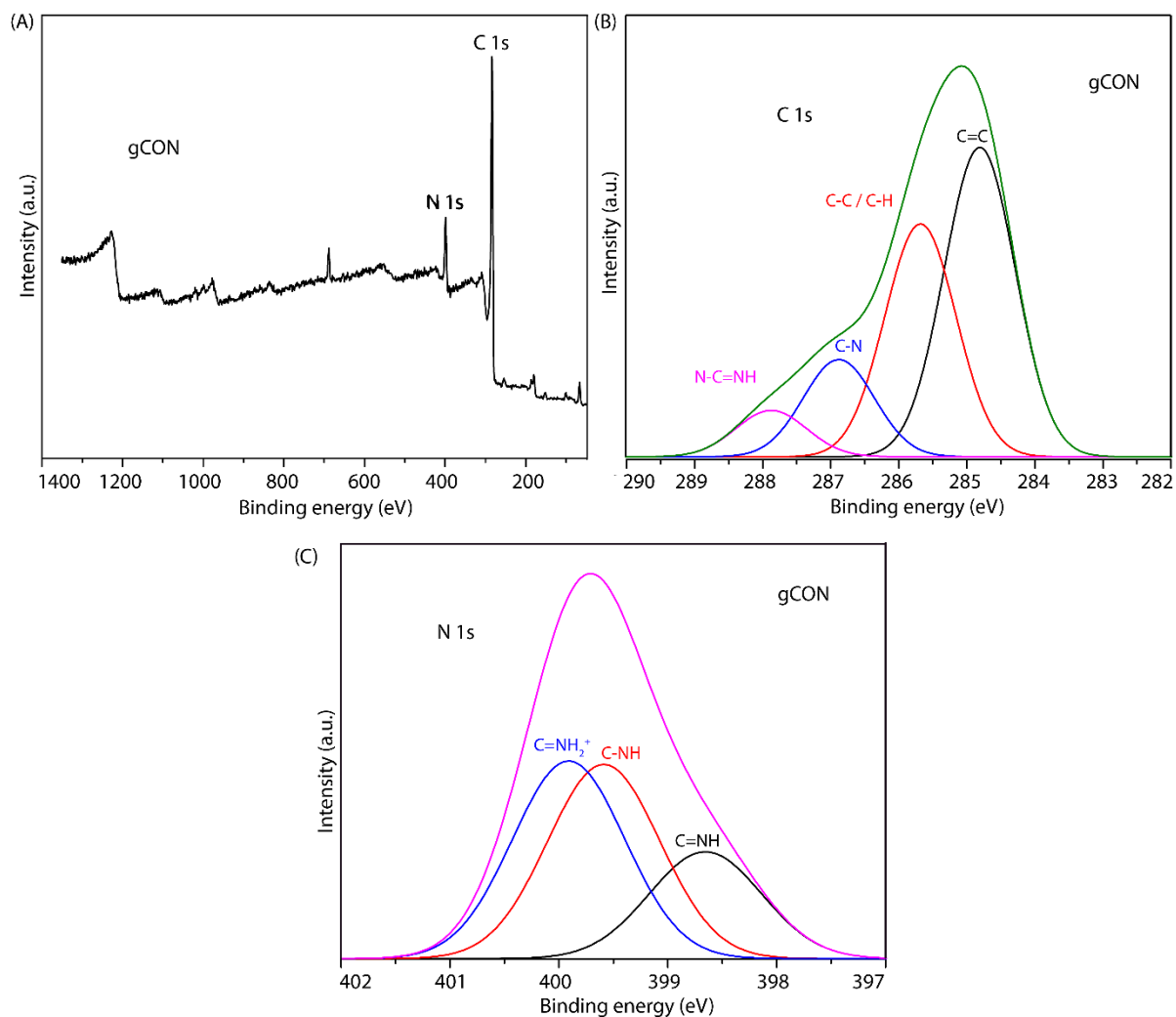


**Fig. S4.** The X-ray photoelectron spectroscopy (XPS) analysis of gCONs. XPS data profile: wide scan of gCONs (A), the deconvoluted peak of C 1s (B), and N 1s (C).

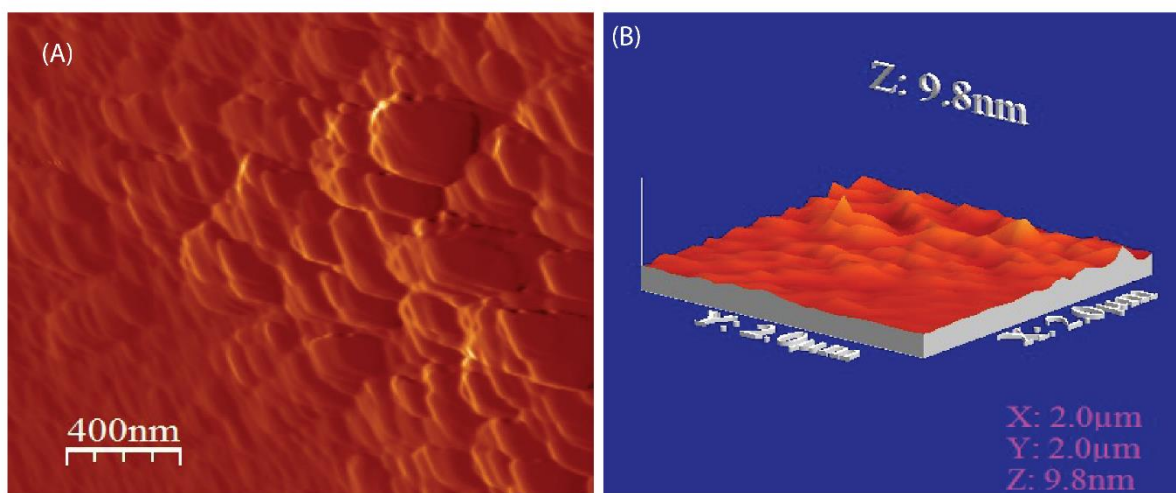


**Fig. S5.** AFM topographic scans corresponding to the height profile (A) and 3-D height image (B).

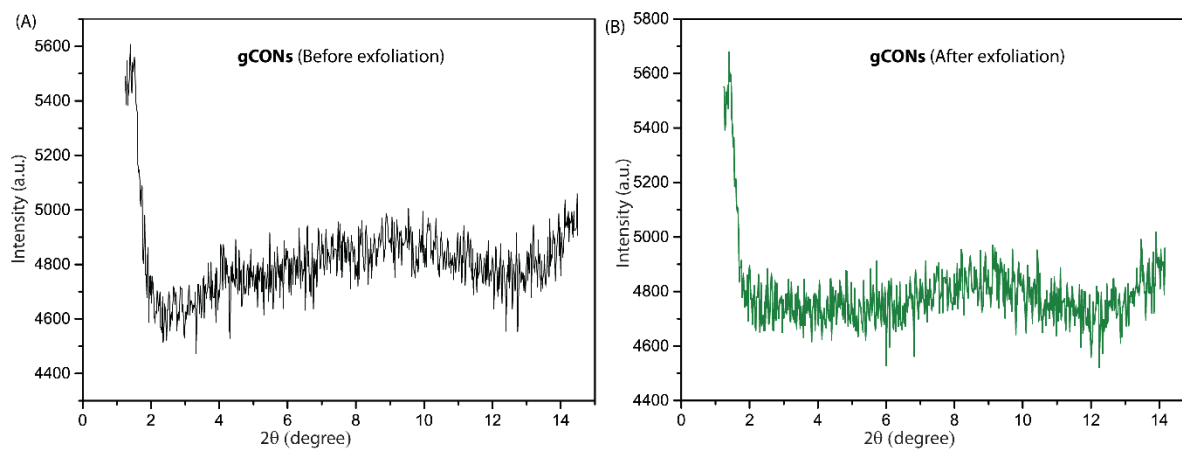


**Fig. S6.** Low angle PXRD analyses of gCONs before (A) and after ((B) exfoliation by sonication for 20 min in the aqueous solution.

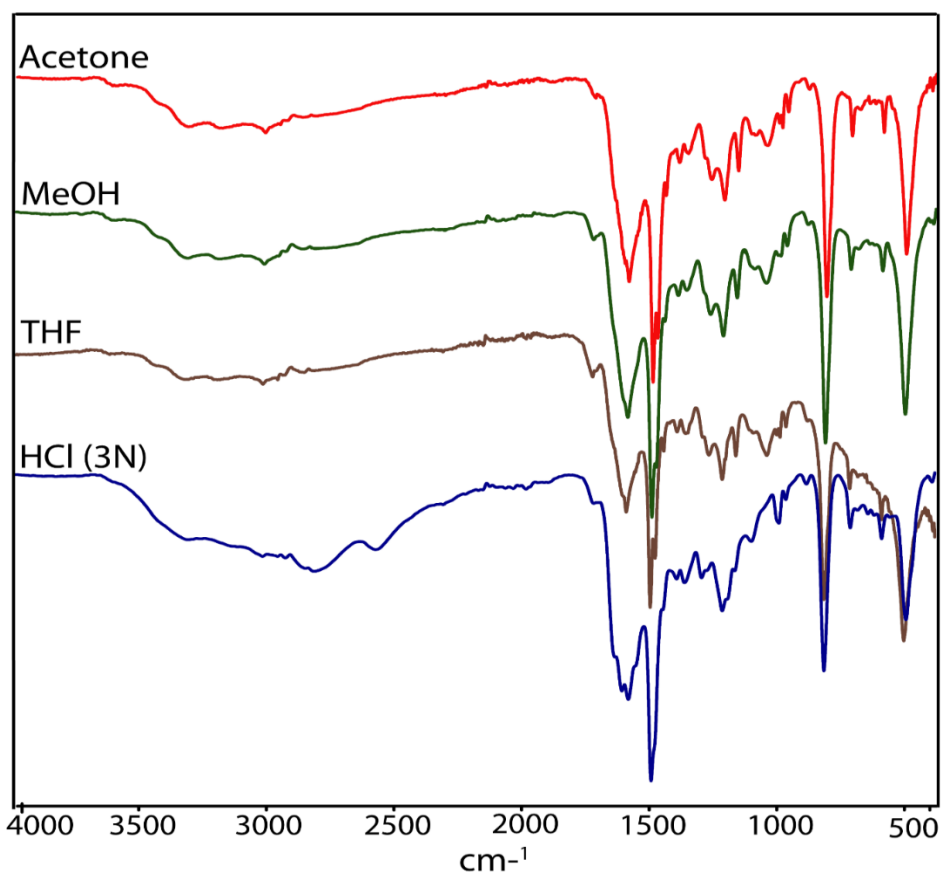


**Fig. S7.** FT-IR spectra of gCONs after the treatment (for 10 days) with acetone, methanol, tetrahydrofuran (THF), and HCl (3N) solution. No significant alterations in FT-IR spectra of gCONs denote its structural stability under these conditions.

### 3. Details of the DFT calculations:

All the calculations in this study have been performed with density functional theory (DFT), with the aid of the Turbomole 7.2 suite of programs,<sup>6</sup> using the PBE functional,<sup>7</sup> with dispersion correction<sup>8</sup> and m4 grid size. The TZVP basis set has been employed.<sup>9</sup> The resolution of identity (RI),<sup>10</sup> along with the multipole accelerated resolution of identity (marij) approximations,<sup>11</sup> have been employed to accurately and efficiently treat the electronic Coulomb term in the DFT calculations. A solvent correction was incorporated with optimization calculations using the COSMO model,<sup>12</sup> with water ( $\epsilon = 78.355$ ) as the solvent. The values reported are  $\Delta G$  values, with zero-point energy corrections, internal energy, and entropic contributions were included through frequency calculations on the optimized minima, with the temperature taken to be 298.15 K. Harmonic frequency calculations were performed for all stationary points to confirm them as local minima or transition state structures. Monomer

.....  
optimization has performed at the same level of theory without solvent correction, and we have omitted the frequency calculations due to the large size of the structure.

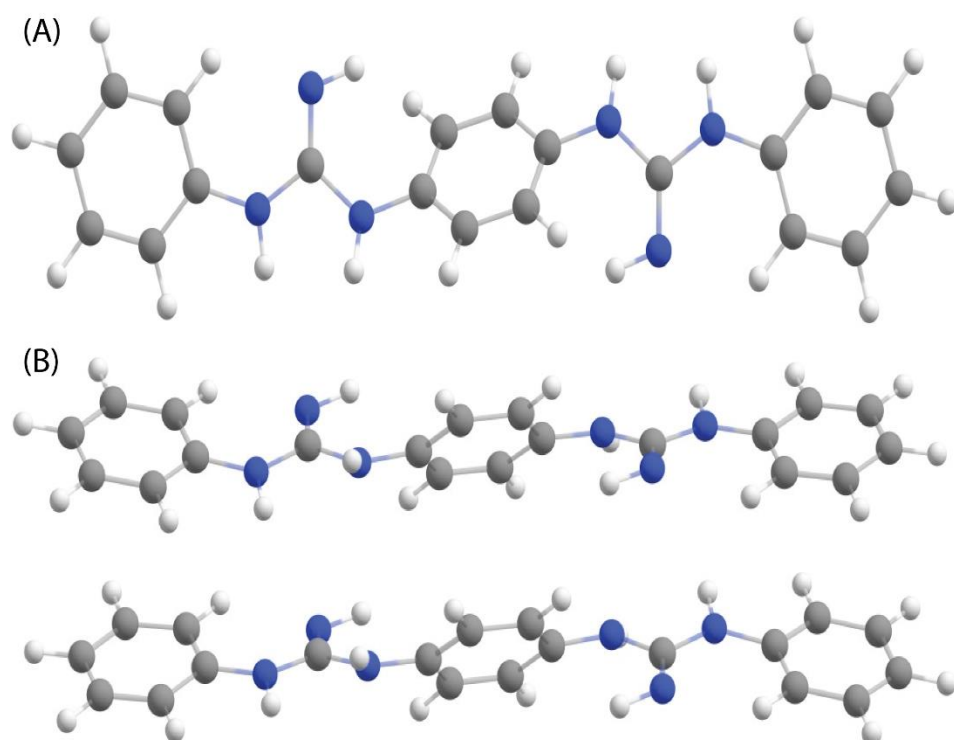


**Fig. S8.** Optimized geometries of two truncated models chosen for the study. (A) Monolayer model, and (B) bilayer model of gCONs. Color scheme: grey represents carbon, white represents hydrogen, and blue represents nitrogen.

**Table S1.** XYZ coordinates of the PBE-D3/TZVP optimized geometries of structures discussed in the manuscript.

(1) Monolayer model:

46

C	-3.275079	0.776953	-2.699320
C	-3.484702	0.305204	-1.399952
C	-2.008366	1.266104	-3.045827
C	-2.460513	0.315333	-0.447011
C	-0.975138	1.278422	-2.111194
C	-1.186379	0.803141	-0.798205

---

H	-4.466560	-0.076954	-1.111247
H	-1.820164	1.640722	-4.054191
H	-2.630329	-0.036052	0.568127
H	0.011318	1.656665	-2.392984
N	-0.090081	0.847184	0.072632
H	0.752175	1.256330	-0.325440
C	0.024604	0.435687	1.391681
N	-0.998637	0.128722	2.121495
H	-0.681038	-0.227070	3.029853
N	1.375356	0.435717	1.784219
H	2.038041	0.158407	1.061518
C	1.824809	0.240904	3.105140
C	2.930104	-0.592645	3.346551
C	1.233288	0.906342	4.194420
C	3.436095	-0.759265	4.634451
C	1.739379	0.740098	5.481905
C	2.845680	-0.092330	5.723297
H	3.391865	-1.129543	2.514654
H	0.396470	1.587436	4.033707
H	4.271813	-1.441741	4.795151
H	1.277564	1.277093	6.313732
N	3.296109	-0.281439	7.044970
H	2.632021	0.000580	7.764556
C	4.646016	-0.268966	7.439559
N	5.670235	0.022292	6.704492
H	5.354329	0.354627	5.786785
N	4.759203	-0.647884	8.768627
H	3.912228	-1.032348	9.180989
H	-4.084422	0.767678	-3.431318
C	5.850889	-0.571167	9.643177
C	5.623352	-0.965039	10.980259
C	7.136303	-0.129592	9.272453

---

C	6.651495	-0.917711	11.919303
C	8.155263	-0.083122	10.229975
C	7.929328	-0.473745	11.553267
H	4.628018	-1.306405	11.277480
H	7.317635	0.160533	8.240121
H	6.450443	-1.228189	12.946785
H	9.145981	0.262396	9.925749
H	8.734420	-0.436735	12.289093

(2) Bilayer model:

92

C	-3.395406	0.816029	-2.724196
C	-3.584971	0.204755	-1.481977
C	-2.221452	1.547054	-2.946715
C	-2.630379	0.311767	-0.464983
C	-1.257329	1.655434	-1.949444
C	-1.450082	1.043293	-0.693087
H	-4.497971	-0.363486	-1.288428
H	-2.056729	2.045183	-3.904268
H	-2.786860	-0.145570	0.509344
H	-0.349533	2.237128	-2.129192
N	-0.434935	1.216795	0.255947
H	0.301703	1.859490	-0.024600
C	-0.271634	0.653293	1.510474
N	-1.217148	0.024384	2.130521
H	-0.843990	-0.386091	2.994027
N	1.034865	0.881292	1.976515
H	1.758672	0.861377	1.260088
C	1.488333	0.579978	3.275971
C	2.733053	-0.044800	3.447687
C	0.760460	0.950340	4.420709
C	3.259165	-0.265186	4.720024
C	1.287830	0.740084	5.690321

---

C	2.550406	0.145776	5.863354
H	3.299296	-0.367081	2.570617
H	-0.203422	1.448805	4.317768
H	4.211315	-0.787643	4.815871
H	0.724811	1.072345	6.565548
N	3.033340	-0.062434	7.167969
H	2.339972	0.077085	7.901069
C	4.372254	0.074345	7.576192
N	5.366541	0.499207	6.868683
H	5.024628	0.844163	5.966342
N	4.513284	-0.344663	8.891586
H	3.725110	-0.870387	9.262385
H	-4.153228	0.734034	-3.505562
C	5.626683	-0.290391	9.743926
C	5.493852	-0.915381	11.002019
C	6.834995	0.359138	9.429563
C	6.542867	-0.894090	11.919005
C	7.874761	0.374608	10.362784
C	7.745102	-0.248015	11.606777
H	4.555802	-1.416709	11.256497
H	6.933030	0.850690	8.465079
H	6.415694	-1.382597	12.887671
H	8.797640	0.902014	10.111847
H	8.563083	-0.222512	12.328911
C	-3.543690	4.829951	-1.960395
C	-3.659446	4.171097	-0.733740
C	-2.345164	5.485494	-2.266799
C	-2.609551	4.160015	0.188009
C	-1.286218	5.480798	-1.361052
C	-1.405013	4.819172	-0.120471
H	-4.579745	3.637130	-0.487418
H	-2.229178	6.002469	-3.221982

---

H	-2.697450	3.641575	1.139286
H	-0.351258	5.990118	-1.611028
N	-0.282237	4.848688	0.720890
H	0.503188	5.382360	0.355597
C	-0.131477	4.403794	2.026583
N	-1.121567	3.969657	2.734691
H	-0.773253	3.605766	3.627053
N	1.211570	4.525947	2.425748
H	1.899396	4.395278	1.685786
C	1.702785	4.308834	3.725584
C	2.966965	3.714887	3.887582
C	1.000310	4.712366	4.875537
C	3.503525	3.500726	5.152990
C	1.535860	4.488742	6.143069
C	2.783772	3.867503	6.303940
H	3.524296	3.386784	3.007214
H	0.045883	5.232057	4.788387
H	4.468735	3.002943	5.247173
H	0.975116	4.807139	7.025087
N	3.249087	3.569664	7.600515
H	2.528609	3.585907	8.320334
C	4.553152	3.823058	8.059814
N	5.490429	4.449831	7.425329
H	5.112458	4.835956	6.552765
N	4.724764	3.289150	9.326161
H	3.992281	2.650546	9.626136
H	-4.370129	4.826382	-2.673243
C	5.740090	3.494667	10.268625
C	5.545234	2.929300	11.546358
C	6.923574	4.212207	10.013746
C	6.510405	3.069176	12.538777
C	7.879300	4.351428	11.025785

---

C	7.687635	3.786199	12.289384
H	4.634984	2.358413	11.747040
H	7.081228	4.634144	9.023772
H	6.343724	2.607059	13.513941
H	8.795045	4.907896	10.811644
H	8.446534	3.892985	13.066755

(3)  $[\text{HPO}_4]^{2-}$  ion

6

O	-0.124895	1.238992	1.323964
P	-0.097313	1.369002	3.056195
O	-1.439673	0.672884	3.439482
O	1.192607	0.602773	3.500368
O	-0.048570	2.903757	3.355955
H	0.721667	1.593517	0.996298

(4)  $\text{HPO}_4^{2-}$  with the monolayer model:

52

C	-2.865139	1.182694	-2.937649
C	-3.163861	0.618912	-1.692991
C	-1.561919	1.645246	-3.172001
C	-2.195076	0.511947	-0.688930
C	-0.581896	1.541874	-2.187426
C	-0.879669	0.969135	-0.925028
H	-4.174730	0.256635	-1.488923
H	-1.303899	2.090729	-4.135888
H	-2.433189	0.086961	0.283945
H	0.435431	1.898807	-2.370099
N	0.169772	0.900711	-0.008567
H	1.086338	1.299122	-0.358056
C	0.207163	0.294169	1.235931
N	-0.869493	-0.065921	1.878848
H	-0.599745	-0.569329	2.730752
N	1.529228	0.137761	1.657172

---

H	2.259672	-0.012656	0.897116
C	1.959853	-0.123184	2.956116
C	3.193015	-0.792972	3.126593
C	1.274276	0.301048	4.115511
C	3.717297	-1.029249	4.394043
C	1.811839	0.074447	5.382954
C	3.033306	-0.596014	5.544275
H	3.735903	-1.124562	2.238924
H	0.339450	0.855771	4.031953
H	4.655932	-1.577948	4.492791
H	1.274482	0.433889	6.264252
N	3.536936	-0.859296	6.843291
H	2.828994	-0.864291	7.576443
C	4.818267	-0.462340	7.260932
N	5.700692	0.174856	6.560265
H	5.288340	0.445676	5.659980
N	5.056485	-0.882793	8.562300
H	4.365665	-1.526094	8.941878
H	-3.631398	1.264305	-3.710989
C	6.087705	-0.546153	9.447007
C	6.019185	-1.097482	10.745775
C	7.166254	0.301320	9.124075
C	6.999062	-0.808806	11.693143
C	8.138354	0.584208	10.089379
C	8.069528	0.037864	11.374652
H	5.184719	-1.754551	11.006129
H	7.228646	0.715928	8.120463
H	6.922903	-1.248165	12.690118
H	8.966890	1.244354	9.821927
H	8.836975	0.263950	12.117070
O	2.501226	1.934882	-1.031455
P	3.527249	0.778855	-1.316647

---

O	3.416675	-0.355393	-0.230406
O	3.001862	0.055290	-2.784622
O	4.967005	1.232270	-1.656121
H	2.071479	-0.212834	-2.669031

(5)  $\text{HPO}_4^{2-}$  with the bilayer model (mode-1)

98

C	0.214602	-1.423169	-9.191791
C	-0.790933	-1.927288	-8.360473
C	1.346739	-0.841159	-8.604465
C	-0.686181	-1.863956	-6.968561
C	1.468773	-0.772692	-7.219244
C	0.453234	-1.282344	-6.375604
H	-1.687661	-2.370281	-8.801217
H	2.143707	-0.435023	-9.232280
H	-1.474560	-2.239007	-6.320298
H	2.349394	-0.310919	-6.764608
N	0.653270	-1.147836	-5.006712
H	1.496054	-0.604006	-4.719094
C	-0.017670	-1.736129	-3.946219
N	-1.103053	-2.442249	-4.087313
H	-1.377525	-2.812749	-3.170623
N	0.670989	-1.491693	-2.761796
H	1.594316	-1.024824	-2.873741
C	0.230844	-1.765824	-1.459284
C	1.158904	-2.234653	-0.513754
C	-1.089674	-1.530669	-1.031819
C	0.803216	-2.426893	0.820741
C	-1.443224	-1.706409	0.302350
C	-0.503033	-2.135843	1.255996
H	2.180078	-2.452575	-0.833807
H	-1.822976	-1.128085	-1.732421
H	1.542969	-2.837846	1.507652

---

H	-2.459440	-1.463311	0.622740
N	-0.928260	-2.304017	2.587069
H	-1.936920	-2.242381	2.712564
C	-0.160426	-2.136391	3.746419
N	1.060193	-1.718276	3.830387
H	1.374959	-1.392939	2.911946
N	-0.895578	-2.513701	4.865669
H	-1.804804	-2.926270	4.671457
H	0.117309	-1.474336	-10.278079
C	-0.556792	-2.488582	6.225117
C	-1.575815	-2.834320	7.140919
C	0.721513	-2.162391	6.720915
C	-1.316936	-2.874165	8.509841
C	0.960405	-2.202367	8.098077
C	-0.043200	-2.561218	9.001928
H	-2.573596	-3.078864	6.766240
H	1.500567	-1.881108	6.016630
H	-2.120957	-3.146904	9.196779
H	1.954565	-1.938818	8.465445
H	0.156924	-2.584101	10.074459
C	-2.641826	1.433620	-7.936803
C	-3.481225	1.226156	-6.838436
C	-1.295322	1.745023	-7.706278
C	-3.003233	1.320604	-5.527037
C	-0.804714	1.847709	-6.408926
C	-1.648434	1.635774	-5.293756
H	-4.533739	0.976599	-6.997624
H	-0.612413	1.885406	-8.546673
H	-3.651989	1.143880	-4.672051
H	0.251562	2.070051	-6.237228
N	-1.066094	1.778785	-4.037167
H	-0.035582	1.928379	-4.032527

---

C	-1.612607	1.603627	-2.774977
N	-2.838119	1.206234	-2.584511
H	-3.012962	1.112561	-1.580627
N	-0.656574	1.925806	-1.808329
H	0.313307	2.008134	-2.191449
C	-0.762058	1.785175	-0.421336
C	0.399905	1.428224	0.296322
C	-1.946665	2.024685	0.303528
C	0.361545	1.257447	1.675632
C	-1.978689	1.847659	1.687977
C	-0.836105	1.444155	2.390589
H	1.331995	1.253444	-0.253904
H	-2.840920	2.402006	-0.192788
H	1.262920	0.939238	2.201629
H	-2.906619	2.039271	2.232614
N	-0.918570	1.197130	3.780255
H	-1.854374	0.996810	4.127607
C	-0.030539	1.722005	4.724491
N	0.922935	2.571720	4.508492
H	0.869961	2.900403	3.537168
N	-0.285119	1.189895	5.981999
H	-0.819469	0.323724	5.984516
H	-3.023616	1.341907	-8.955463
C	0.072316	1.664069	7.249190
C	-0.433839	0.958550	8.361647
C	0.881367	2.795979	7.472531
C	-0.138970	1.370629	9.658422
C	1.159087	3.202449	8.781976
C	0.658132	2.501009	9.883248
H	-1.051789	0.071901	8.199891
H	1.290143	3.329611	6.617076
H	-0.536544	0.800524	10.501011

---

H	1.786920	4.083277	8.936618
H	0.888049	2.824318	10.900167
O	4.162596	2.125729	-3.912788
P	2.881712	1.371228	-3.068178
O	2.867005	-0.050410	-3.735484
O	3.256624	1.379215	-1.562467
O	1.602078	2.230016	-3.389733
H	4.325337	2.990653	-3.493086

(6)  $\text{HPO}_4^{2-}$  with the bilayer model (mode-2)

98

C	-1.221678	-2.248759	-8.429611
C	-1.928446	-2.824296	-7.370246
C	-0.061455	-1.516404	-8.142321
C	-1.499463	-2.685574	-6.045079
C	0.382973	-1.370737	-6.832556
C	-0.328747	-1.952566	-5.755509
H	-2.839842	-3.394705	-7.570008
H	0.495430	-1.033212	-8.948281
H	-2.051400	-3.132162	-5.221220
H	1.270096	-0.776028	-6.606068
N	0.188894	-1.734573	-4.476588
H	1.043581	-1.132388	-4.472504
C	-0.246370	-2.239038	-3.263892
N	-1.257520	-3.063359	-3.173665
H	-1.372725	-3.337967	-2.192302
N	0.530795	-1.798314	-2.199070
H	1.408443	-1.242446	-2.348067
C	0.228797	-2.023552	-0.845016
C	1.270319	-2.356408	0.037751
C	-1.064189	-1.856804	-0.311910
C	1.043111	-2.496965	1.406588
C	-1.291777	-1.985389	1.054581

---

C	-0.242849	-2.292683	1.938073
H	2.276618	-2.494829	-0.361833
H	-1.884958	-1.554219	-0.963103
H	1.868017	-2.795393	2.054810
H	-2.293230	-1.802134	1.451886
N	-0.521704	-2.424332	3.314379
H	-1.515042	-2.479927	3.533676
C	0.289129	-1.937247	4.354239
N	1.394132	-1.276492	4.242349
H	1.556021	-1.046257	3.256828
N	-0.250093	-2.290877	5.584911
H	-0.993016	-2.984946	5.546904
H	-1.571484	-2.357128	-9.458452
C	0.155892	-1.947482	6.882454
C	-0.552480	-2.541600	7.949090
C	1.196264	-1.045391	7.174737
C	-0.225280	-2.244331	9.270636
C	1.507843	-0.756315	8.505666
C	0.810243	-1.347903	9.561784
H	-1.367485	-3.237722	7.731241
H	1.732309	-0.578876	6.352290
H	-0.790054	-2.714397	10.078693
H	2.304929	-0.039314	8.713870
H	1.059589	-1.107439	10.596847
C	-1.177385	1.882822	-8.683691
C	-2.158902	1.499696	-7.764615
C	0.089872	2.244485	-8.206214
C	-1.905183	1.484219	-6.390366
C	0.361594	2.229930	-6.841083
C	-0.632611	1.852733	-5.908125
H	-3.146060	1.193942	-8.120357
H	0.878222	2.534730	-8.905270

---

H	-2.661340	1.170771	-5.674405
H	1.356085	2.496174	-6.473511
N	-0.271543	1.900026	-4.564526
H	0.740328	2.048595	-4.383986
C	-0.992622	1.560306	-3.427085
N	-2.228902	1.159821	-3.462626
H	-2.528916	0.909711	-2.516069
N	-0.184411	1.743026	-2.304031
H	0.836524	1.802646	-2.517904
C	-0.521055	1.612407	-0.957763
C	0.510148	1.249229	-0.063530
C	-1.798866	1.879779	-0.426771
C	0.269667	1.138856	1.299409
C	-2.035036	1.758534	0.944713
C	-1.013835	1.375707	1.823360
H	1.489619	0.990851	-0.476737
H	-2.607130	2.234684	-1.066136
H	1.072310	0.816118	1.963281
H	-3.032419	1.972066	1.337348
N	-1.295146	1.171914	3.195571
H	-2.271462	0.971033	3.404337
C	-0.577104	1.786337	4.231782
N	0.380064	2.648873	4.102019
H	0.476071	2.894611	3.109651
N	-1.019943	1.330974	5.464330
H	-1.609348	0.502760	5.429469
H	-1.388323	1.885976	-9.754920
C	-0.772612	1.817706	6.752594
C	-1.469037	1.199788	7.812903
C	0.116294	2.869944	7.043916
C	-1.274511	1.613931	9.126867
C	0.292649	3.280309	8.369588

---

C	-0.393277	2.663058	9.419417
H	-2.147964	0.370675	7.597287
H	0.664476	3.336337	6.228363
H	-1.810362	1.105094	9.930622
H	0.987845	4.097188	8.578500
H	-0.238995	2.986186	10.450698
O	4.658030	0.835064	-3.762192
P	2.990906	0.568676	-3.513868
O	2.578040	-0.255149	-4.767801
O	2.841117	-0.224842	-2.173609
O	2.343858	2.004245	-3.439050
H	4.984688	1.417099	-3.051142

(7) monomer

162

C	0.081184	0.014938	-2.808482
C	0.114217	-1.120329	-1.937482
C	0.091009	1.292494	-2.323698
C	0.170418	-0.890780	-0.521665
C	0.146180	1.563622	-0.919713
C	0.160166	0.451886	-0.012471
C	0.121970	-2.454836	-2.428002
C	0.249548	-2.000289	0.385950
C	0.169972	0.680009	1.404181
C	0.259513	-3.324740	-0.130689
C	0.214003	-3.512773	-1.517091
C	0.380333	-1.723998	1.784598
H	0.182808	-4.534118	-1.903168
C	0.163053	2.887753	-0.400537
C	0.086371	2.011093	1.897781
C	0.103826	3.072257	0.985060
H	0.052241	2.132776	-3.017085
C	0.333570	-0.447915	2.270060

---

H	0.074255	4.093172	1.372629
H	0.454130	-0.271723	3.339294
C	-0.007138	2.319125	3.344175
C	0.833560	3.276834	3.937312
C	-0.977020	1.713426	4.165915
C	0.736866	3.621857	5.284591
C	-1.086484	2.043372	5.511191
C	-0.228959	2.998039	6.093741
H	1.598434	3.760976	3.325937
H	-1.668425	0.987255	3.734381
H	1.385250	4.376104	5.725579
H	-1.853224	1.558999	6.123495
C	0.229319	4.087624	-1.269790
C	1.253331	4.254802	-2.221236
C	-0.694264	5.136611	-1.124531
C	1.336741	5.408695	-2.991450
C	-0.625101	6.302052	-1.886954
C	0.397870	6.448740	-2.839970
H	2.008528	3.475480	-2.340186
H	-1.500550	5.034072	-0.394688
H	2.147937	5.513027	-3.718483
H	-1.337544	7.112895	-1.750590
C	0.289108	-4.522845	0.742407
C	-0.650319	-4.722363	1.769191
C	1.240950	-5.537082	0.531428
C	-0.649651	-5.866031	2.566287
C	1.255604	-6.685289	1.314886
C	0.310849	-6.868075	2.343147
H	-1.416876	-3.964031	1.941169
H	1.991769	-5.411611	-0.251595
H	-1.373084	-5.998247	3.368091
H	2.011188	-7.454913	1.129736

---

C	0.006937	-2.778687	-3.871475
C	0.945679	-3.616151	-4.496536
C	-1.072306	-2.321624	-4.650734
C	0.840220	-3.985337	-5.837378
C	-1.192586	-2.676931	-5.989126
C	-0.236862	-3.509456	-6.604341
H	1.793420	-3.985377	-3.914812
H	-1.839251	-1.695150	-4.191403
H	1.567223	-4.647386	-6.302936
H	-2.045211	-2.310257	-6.568893
N	-0.391358	3.255909	7.462600
H	-1.195588	2.808421	7.893049
N	0.543951	7.571332	-3.668573
H	1.392857	7.586553	-4.226727
N	-0.423389	-3.803500	-7.964929
H	-1.304689	-3.484359	-8.357124
N	0.381489	-8.064565	3.074331
H	1.187076	-8.648348	2.868128
C	0.297355	4.130180	8.295038
N	-0.042218	3.860865	9.647559
H	-0.049186	2.869753	9.883041
C	0.338017	4.701848	10.716953
C	0.897848	4.162175	11.883226
C	0.105896	6.087472	10.668027
C	1.212870	4.959326	12.983190
C	0.448813	6.893040	11.747598
C	1.004633	6.347617	12.921279
H	1.086527	3.086591	11.941113
H	-0.354431	6.531304	9.784463
H	1.617651	4.528882	13.896838
H	0.269256	7.970220	11.683149
N	1.089455	5.039484	7.851282

---

H	1.567498	5.502899	8.631415
N	1.331486	7.239839	13.955857
H	0.998222	8.189600	13.820751
C	1.878115	6.989764	15.207060
N	2.174945	8.203660	15.864206
H	2.672903	8.889948	15.298410
N	2.012783	5.797819	15.677699
H	2.517237	5.815700	16.569432
H	2.619330	8.076029	16.769219
C	-0.409332	-8.518951	4.120328
N	-1.232714	-7.765050	4.756233
H	-1.787291	-8.320505	5.416054
N	-0.135312	-9.895132	4.355398
H	-0.087392	-10.458726	3.508282
C	-0.598939	-10.593981	5.488065
C	-1.156756	-11.874900	5.349744
C	-0.464629	-10.059247	6.781114
C	-1.560306	-12.610967	6.461269
C	-0.871021	-10.792962	7.892248
C	-1.424666	-12.077169	7.754845
H	-1.291912	-12.299529	4.351525
H	-0.010653	-9.077072	6.917569
H	-2.021700	-13.588946	6.321878
H	-0.739622	-10.367177	8.890264
N	-1.878920	-12.769838	8.891198
H	-1.965223	-12.210748	9.737184
C	-1.704252	-14.148145	9.127117
N	-1.009994	-14.995793	8.456704
H	-0.439335	-14.528283	7.744231
N	-2.381646	-14.542339	10.283035
H	-3.336048	-14.197021	10.364445
H	-2.308801	-15.546389	10.430289

---

C	0.343642	-4.579032	-8.822716
N	1.283980	-5.354438	-8.416044
H	1.787954	-5.752758	-9.215282
N	-0.097040	-4.380079	-10.160968
H	-0.251889	-3.403756	-10.406453
C	0.314375	-5.188731	-11.239320
C	0.689796	-4.604175	-12.459357
C	0.305079	-6.591261	-11.144797
C	1.036497	-5.386231	-13.558603
C	0.654890	-7.373341	-12.242036
C	1.026514	-6.788988	-13.464666
H	0.725943	-3.515129	-12.547343
H	-0.007967	-7.070440	-10.216479
H	1.356708	-4.905283	-14.483255
H	0.622114	-8.462252	-12.153550
N	1.430846	-7.604031	-14.537005
H	1.627047	-8.573558	-14.297704
C	1.079125	-7.404207	-15.887020
N	0.247996	-6.559999	-16.383476
H	-0.282416	-6.083234	-15.646451
N	1.743708	-8.314318	-16.711866
H	2.738884	-8.421281	-16.525001
H	1.540402	-8.140902	-17.693550
C	-0.207741	8.738681	-3.730934
N	-1.085019	9.053414	-2.846360
H	-1.590045	9.898300	-3.134441
N	0.174616	9.486798	-4.876321
H	0.272419	8.928119	-5.722535
C	-0.262062	10.809996	-5.108789
C	-0.151408	11.795200	-4.112063
C	-0.756844	11.187453	-6.364784
C	-0.547627	13.101739	-4.372333

---

C	-1.124292	12.503502	-6.643814
C	-1.037764	13.480392	-5.637433
H	0.256296	11.536408	-3.134113
H	-0.850948	10.435960	-7.153616
H	-0.462964	13.849339	-3.578222
H	-1.478021	12.795535	-7.630466
N	-1.425512	14.820097	-5.804654
H	-1.174508	15.435289	-5.036646
C	-1.934690	15.466412	-6.922615
N	-1.965442	14.914809	-8.086707
H	-2.458698	15.512402	-8.757169
N	-2.322161	16.783628	-6.593649
H	-2.744196	17.287270	-7.368929
H	-2.880758	16.870064	-5.745373
H	0.542473	-2.556534	2.469440
H	0.057754	-0.152419	-3.88533

**4. Phosphate Adsorption analysis:**

**4.1. Adsorption Experiments** — The phosphate adsorption isotherms of **gCON** were performed using a Metrohm ion chromatograph (792 Basic IC, Switzerland) equipped with a METROSEP A Supp 5-250/4.0 (6.1006.530) separation column (4 mm × 100 mm) at various phosphate solution concentrations ranging from 20 to 1000 ppm in Milli-Q water. To the 5 mL volume of the different concentrations of phosphate solutions ( $\text{Na}_2\text{HPO}_4$ ), 5 mg of **gCON** polymer was added and sonicated for 20 min. Thereafter, kept the solution constant stirring up to 6 h at room temperature. After that, each solution was centrifuged and then filtered out to remove the polymer. Next, each solution was diluted to maintain the concentration of phosphate ions to 25 ppm. Finally, we measured the phosphate ion concentration before and after adsorption using the ion chromatograph. The eluent was prepared using 2 mmol  $\text{NaHCO}_3$  mixed with 1.3 mmol  $\text{Na}_2\text{CO}_3$  solutions as recommended. The primary standard used for these experiments was PRIMUS multi-anion solution (10 mg/kg ± 0.2% of each ionic species) from Fluka. The adsorption capacity of **gCONs** was calculated by the following Eq. (1).

$$Q_e = \frac{C_0 - C_e}{m} V \dots \dots \dots \text{Eq. (1)}$$

Where,  $Q_e$  = adsorption capacity (mg/g),  $C_0$  = initial concentration,  $C_e$  = equilibrium concentration,  $V$  = volume of solution,  $m$  = amount of adsorbent (mg).

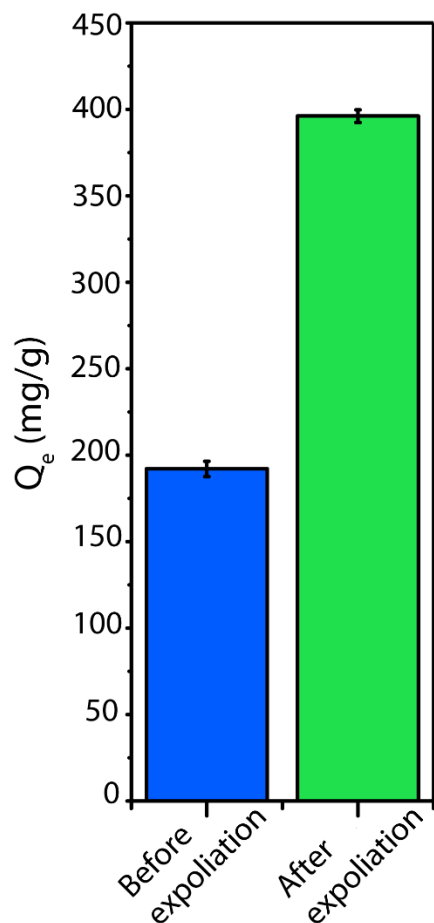


**Fig. S9.** Phosphate adsorption capacity of the gCONs before and after exfoliation by sonication for 20 min in aqueous solution.

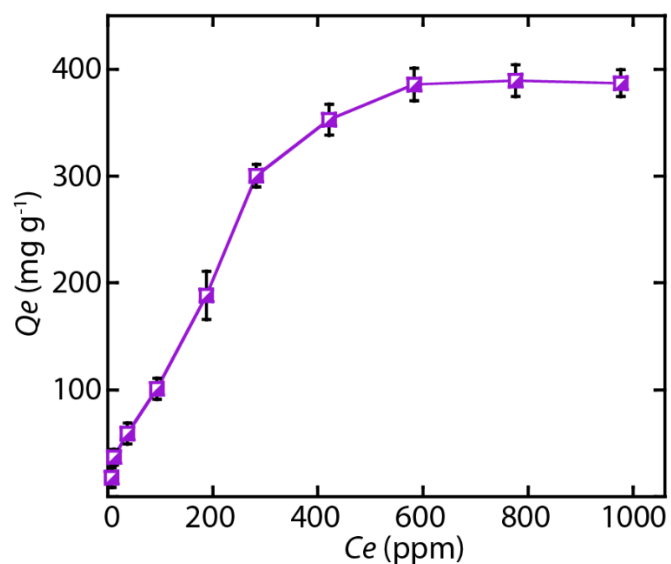


**Fig. S10.** Phosphate ion adsorption isotherm of gCONs (5 mg) at pH 7.0 under room temperature.

**4.2. Adsorption Isotherms** — To explore the adsorption patterns, Langmuir isotherm (Eq.(2)), Freundlich isotherm models (Eq.(3)) were used to fit the adsorption data.

$$Q_e = \frac{Q_m K_l C_e}{1 + K_l C_e} \dots \dots Eq. (2)$$

$$Q_e = K_f C_e^{1/n} \dots \dots Eq. (3)$$

Where  $C_e$  is the equilibrium phosphate ion concentration (ppm),  $Q_e$  is the corresponding adsorption capacity (mg/g). The  $K_l$  is the Langmuir constant, and  $Q_m$  is the max adsorption capacity for the Langmuir model. The  $K_f$  and  $n$  are the Freundlich constants. For Freundlich adsorption isotherm, the  $K_f$  is associated with the adsorption capacity of the gCONs. Whereas,  $1/n$  describes the extent of adsorption (favorable  $1/n < 1$  or unfavorable  $1/n > 2$ ). The data fitted with the Langmuir adsorption isotherm revealed a high  $Q_m$  value of  $537.2 \text{ mg} \cdot \text{g}^{-1}$ , which suggests the exceptional adsorption performance of the gCONs.

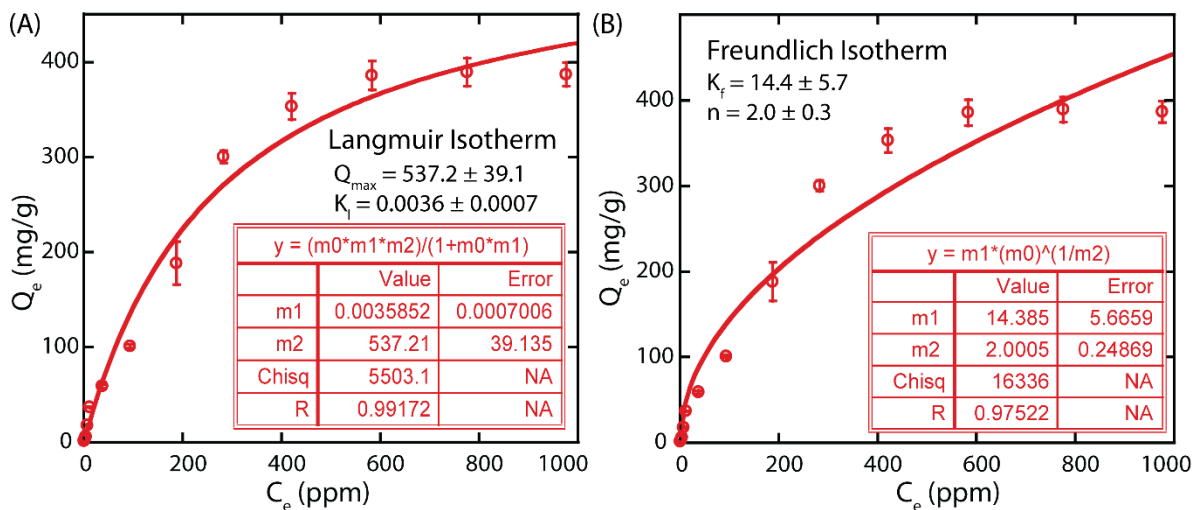


**Fig. S11.** Langmuir (A) and Freundlich (B) isotherm plots of phosphate ion adsorption by gCONs.

**4.3. Time-dependent adsorption study** — To investigate the time-dependent adsorption process, 5 mg of the adsorbent (gCON) was added into 5 mL of Milli-Q water ( $\text{pH} \approx 7$ ) and sonicated the solution for 20 minutes to exfoliate the polymer. Thereafter, 5 mg of solid  $\text{Na}_2\text{HPO}_4$  was added to make the final concentrations of phosphate 1000 ppm. Then, different time interval (2, 4, 6, 8, 10, 20, 30, 40 and 60 minutes) solutions were collected and centrifuged and then filtered out to remove the polymer. Next, each solution was diluted to maintain the concentration of phosphate ions to 25 ppm. Finally, we measured the phosphate ion concentration before and after adsorption using the ion chromatograph. To explore the

adsorption mechanism, the time-dependent adsorption data was fitted with the pseudo-first-order kinetics model and the pseudo-second-order kinetics model described in Eq. (4) and (5), respectively:

$$\ln(Q_e - Q_t) = \ln Q_e - k_1 t \dots \text{Eq. (4)}$$

$$\frac{t}{Q_t} = \frac{1}{k_2 Q_e^2} + \frac{t}{Q_e} \dots \text{Eq. (5)}$$

Where  $Q_t$  and  $Q_e$  (mg/g) are the adsorption capacities of phosphate at time  $t$  and at equilibrium, respectively. The  $k_1$  and  $k_2$  (g/mg·min) are the adsorption rate constants of the pseudo-first-order equation and the pseudo-second-order equation, respectively.<sup>13</sup>

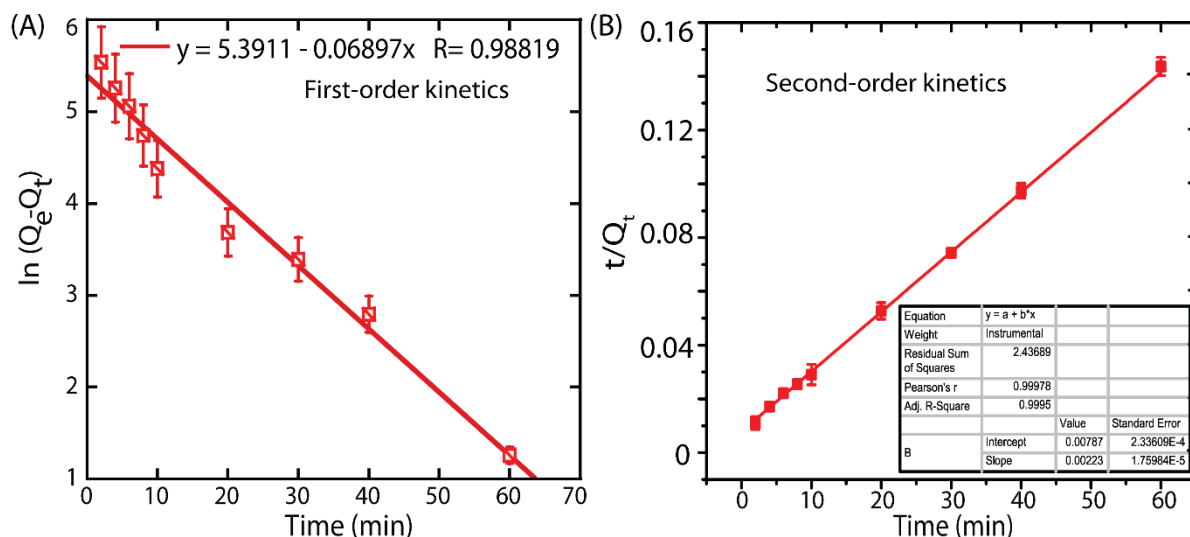


**Fig. S12.** Time-dependent adsorption efficiency of gCONs fitted with the first-order (A) and second-order (B) kinetic models.

**4.4. Kinetics study with different amount of gCON** — The phosphate adsorption rate was measured using different initial concentrations of gCON. To the 5 mL volume of Milli-Q water ( $\text{pH} \approx 7$ ) different amount (1, 3, 5, 7 and 10 mg) of gCON polymer was added respectively and sonicated all the different solution for 20 minutes to exfoliate the polymer and thereafter, 5 mg of solid  $\text{Na}_2\text{HPO}_4$  was added respectively to make the final concentrations of phosphate 1000 ppm. Then, at different time interval (2, 4, 6, 8, 10, 20, 30, 40 and 60 minutes) solution were collected and centrifuged and then filtered out to remove the polymer. Next, each solution was

diluted to maintain the concentration of phosphate ions to 25 ppm. Finally, we measured the phosphate ion concentration before and after adsorption using the ion chromatograph.

**4.5. Anion Selectivity Study** — To evaluate the competing effect of coexisting ions on phosphate ion adsorption, 5 mg of the gCONs were added to the different concentrations of the sodium salt (0.25 mM) of different anions (NaF, NaCl, NaNO<sub>3</sub>, Na<sub>2</sub>HPO<sub>4</sub>, Na<sub>2</sub>SO<sub>4</sub>). The chromatogram results indicate that more than 85% of initial phosphate was adsorbed on gCON.

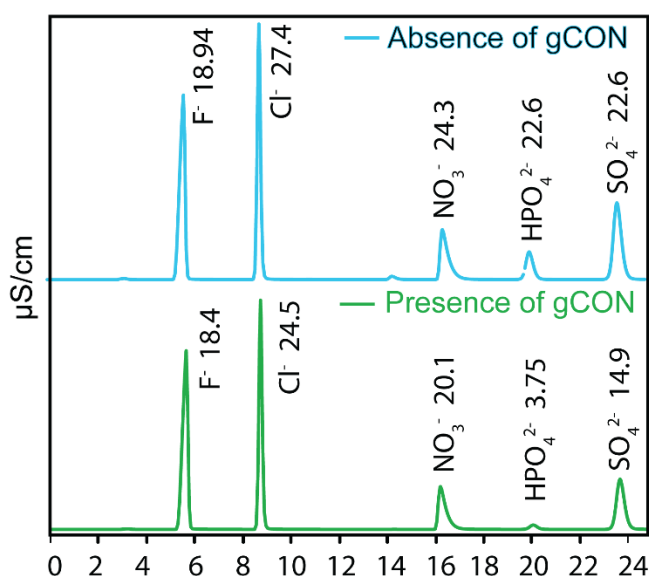


**Fig. S13.** Ion chromatograms in the absence and presence of gCONs.

**Table S2.** Ion chromatographic analysis demonstrates the concentrations of different competitive anions present before and after the treatment of gCONs. The concentration of all anions was 0.25 mM for the anion selectivity analysis.

	Concentration (ppm)				
	F <sup>-</sup>	Cl <sup>-</sup>	NO <sub>3</sub> <sup>-</sup>	HPO <sub>4</sub> <sup>2-</sup>	SO <sub>4</sub> <sup>2-</sup>
Before adsorption	18.94	27.4	24.3	22.6	22.6
After adsorption	18.4	24.5	20.1	3.8	14.9

**Note:** The relative % ion adsorption was calculated based on mass ratio (different anions were taken in mg/L) and calculated using the following equation-

Percentage of adsorption -

$$Q_{ad}(\%) = \frac{(C_o - C_e)}{C_o} * 100\%, \text{ Where, } C_o, C_e \text{ in ppm(mg/L).}$$

**4.6. Influence of pH on phosphate adsorption** — To check the pH-dependency of phosphate ion adsorption by gCONs, five different sets of pH values were selected for the adsorption experiments: pH 4, 6, 7, 8, and 10. The ion chromatogram-based assay was performed in these solutions. The results obtained from chromatogram clearly indicate that in acidic condition, our gCON have the highest phosphate adsorption efficacy and in basic condition at pH 10 adsorption capacity very low.

**4.7. Recyclability test** — The gCONs were regenerated by keeping the phosphate-loaded compound (5 mg) for 24 h in NaOH (0.5 N) solution, and thereafter, it was washed by Milli-Q water for the removal of the remaining NaOH. Recyclability of the regenerated compound was performed with 5 mL, 1100 ppm of phosphate solution. After 24 h, the concentrations of the post-capture phosphate solutions were obtained by ion chromatography techniques. A similar experiment was repeatedly performed for up to 7 cycles. The results obtained from the chromatogram clearly indicate that our gCON had >83-87 % efficiency after 7<sup>th</sup> cycle.

**4.8. Regeneration of gCON** — In an effort to test the recyclability of the sample, 5 mg of the sample was added into 5 mL of a 1000 ppm phosphate (pH  $\approx$  7.0) solution for 24 h. Afterward, NaOH (0.5 N) was used as the eluent to remove the load phosphate. The regenerated sample was washed by Milli-Q water to remove the remaining NaOH solution until pH 7.0 and confirmed by FT-IR spectroscopy and then reused in the succeeding cycle.

**4.9. Retrieval of phosphate ion** — The retrieval of phosphate ions was performed by both absorption and desorption analyses.

**4.10. Adsorption study** — To the 5 ml volume of 1000 ppm phosphate ( $\text{Na}_2\text{HPO}_4$ ) solutions gCON polymer (5 mg) was added, and the solution was kept for 6 h under constant stirring conditions. Thereafter, the solution was centrifuged and then filtered out to get the only phosphate-containing solution. After that, the solution was diluted by 40-times to achieve 25 ppm concentration. Finally, we checked the individual anion concentration before and after adsorption studies by the ion chromatographic technique. It was found that the sorption 394 mg/g.

.....

**4.11. Desorption study** — To the phosphate-loaded **gCON** (5 mg) was stirred with NaOH solution (5 mL of 0.5(N)) at room temperature for 6 h. Thereafter, the solution was centrifuged and filtered out to get the only phosphate-containing solution. Thereafter, the solution was diluted by 40-times to maintain 25 ppm concentration. Finally, we measured the phosphate ion concentration was determined by the ion chromatographic technique. The desorption of phosphate was found 378 mg/g. Therefore, the material has the capacity to reclaim the phosphate ion ~95 percent.

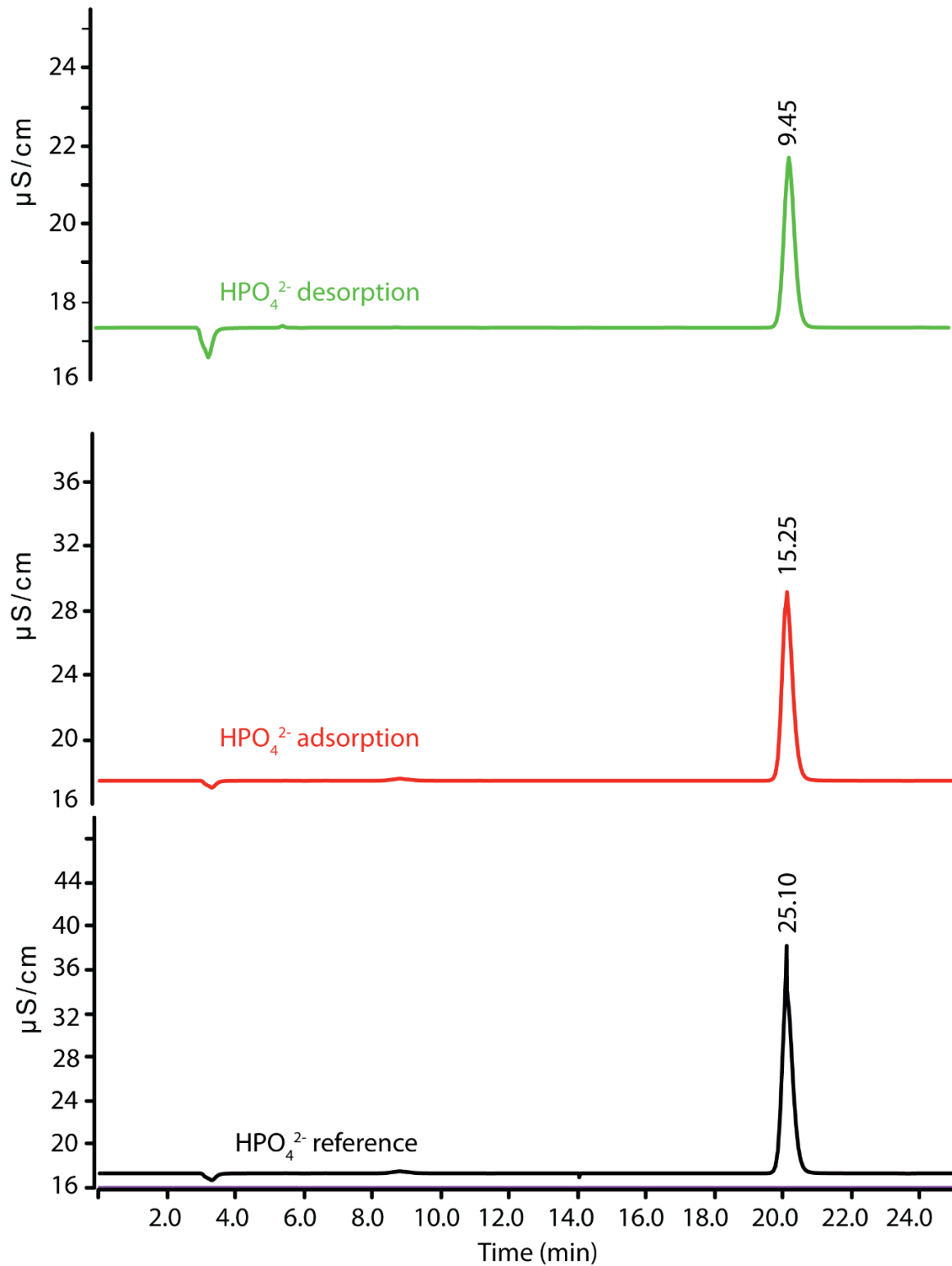


**Fig. S14.** Ion chromatograms after phosphate ion adsorption and desorption (from recovered phosphate ion-containing solution).

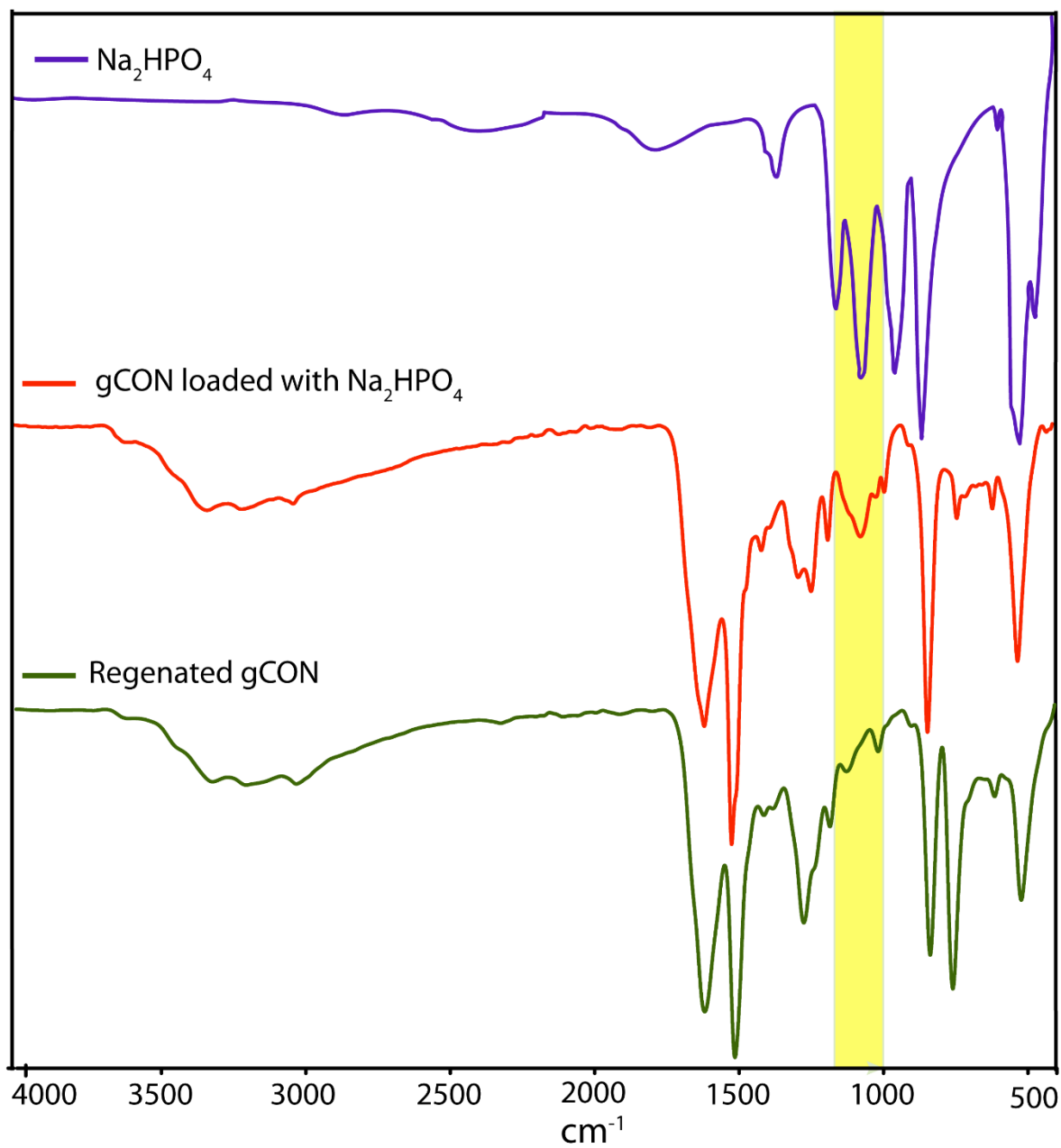


**Fig. S15.** FT-IR of  $\text{Na}_2\text{HPO}_4$ , gCONs loaded with  $\text{Na}_2\text{HPO}_4$ , and regeneration gCONs (after the removal of phosphate ions).

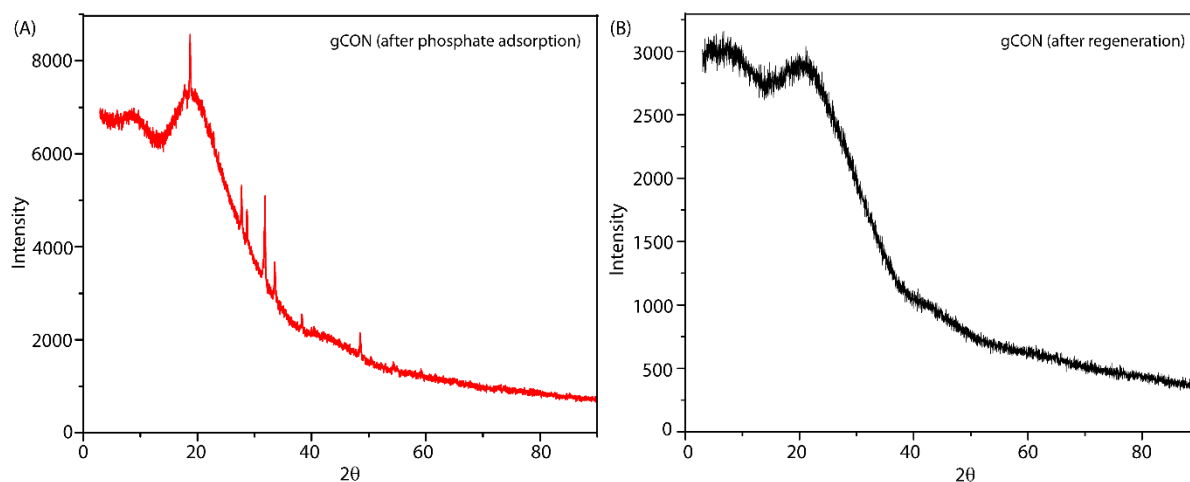


**Fig. S16.** Comparison of PXRD patterns of gCONs after phosphate adsorption (A) and regeneration (B).

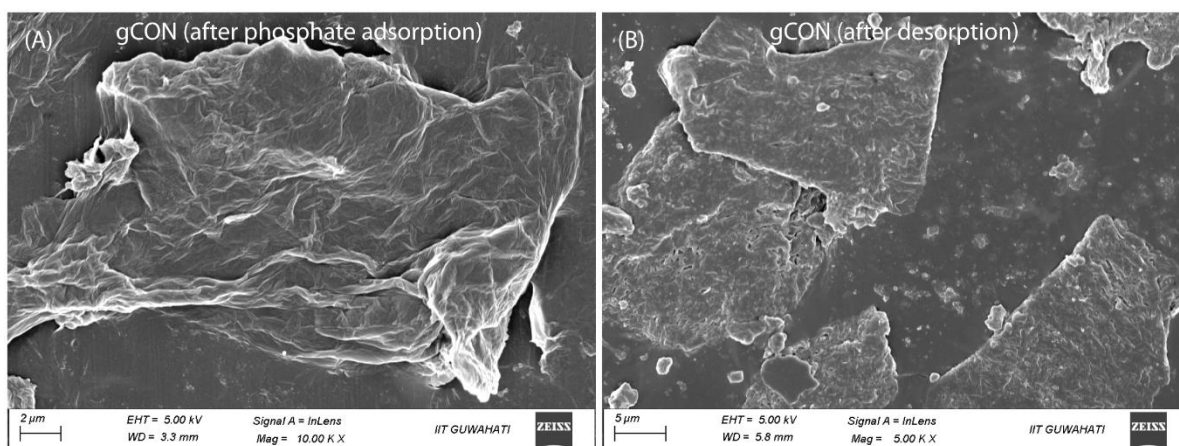


**Fig. S17.** Representative FESEM images of gCONs after phosphate adsorption (A) and regeneration (B).

#### 4.12. Phosphate removal applicability with the real phosphate contaminated wastewater

— To test the practical applicability of the gCONs adsorbent toward phosphate removal in real eutrophic water, the sample was collected from College Nagar, Abhoypur, North Guwahati, Assam, India. All the associated anions with the concentration of phosphate and coexisting species as well as pH are given in Table S3. To the 5 mL volume of the real sample, 5 mg of gCONs polymer was added and sonicated for 20 minutes. After that, the solution was kept for constant stirring up to 6 h at room temperature. Next, the solution was centrifuged and then filtered out to remove the polymer, and subsequently, anions concentration was measured by ion chromatography. The aforementioned study revealed that gCONs effectively reduced phosphate anion concentration in presence of other coexisting anions to below the phosphate

discharge requirement recommended by WHO. These results revealed that the developed gCONs could be utilized as an effective adsorbent to remove phosphate from wastewater.

**Table S3.** Ion chromatographic analysis demonstrating the concentrations of different competitive anions present before and after the treatment of gCONs.

Sample	Existing anions (concentration in ppm)				pH
	F <sup>-</sup>	Cl <sup>-</sup>	HPO <sub>4</sub> <sup>2-</sup>	SO <sub>4</sub> <sup>2-</sup>	
Real eutrophic water	0.411 ± 0.03	24.772 ± 0.07	2.141 ± 0.024	11.126 ± 0.06	6.7
After gCON treatment	0.398 ± 0.02	22.202 ± 0.06	0.414 ± 0.012	8.123 ± 0.05	

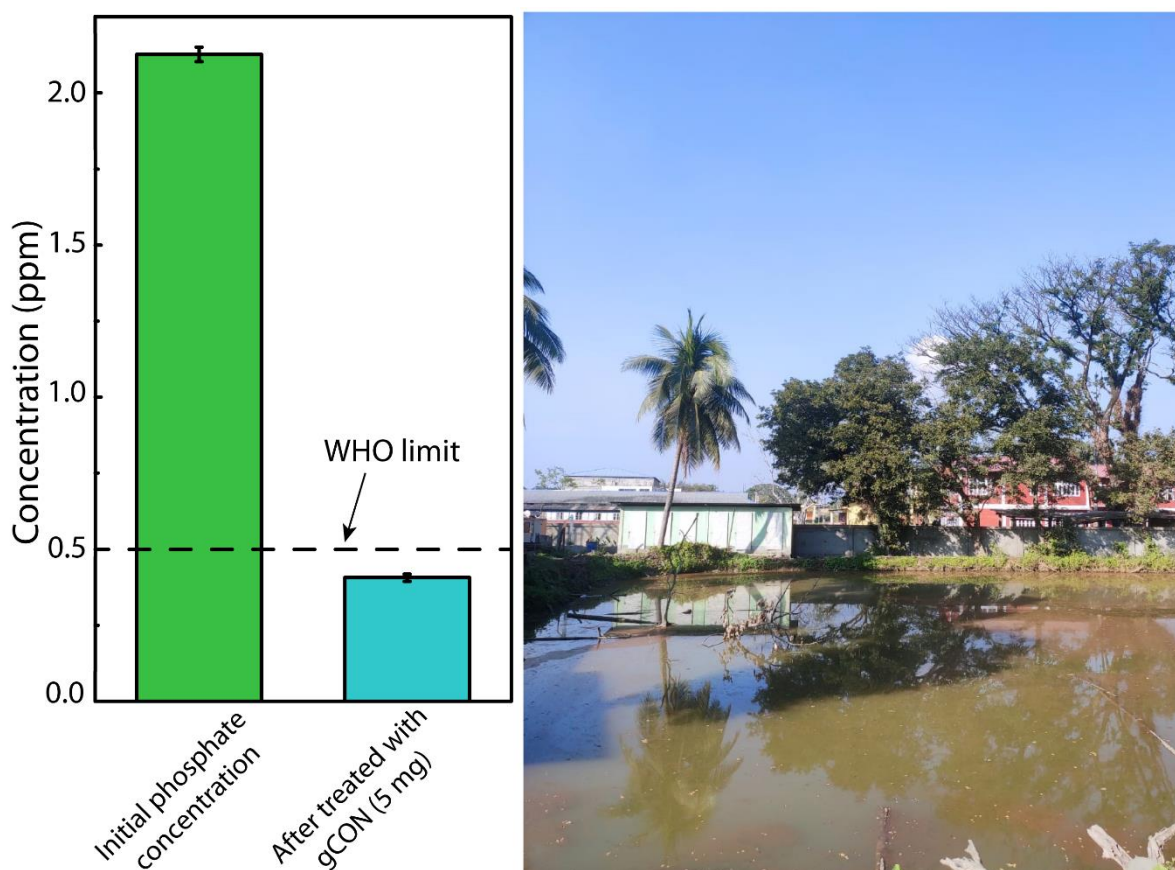


**Fig. S18.** Phosphate ion adsorption capacity of the gCONs from the real phosphate contaminated wastewater. Phosphate contaminated eutrophic water was collected from College Nagar, Abhoypur, North Guwahati, Assam, India.

**Table S4.** Comparison of phosphate adsorption capacity by recently reported materials.

Compound		Adsorption capacity(mg/g)	Equilibrium time	phosphate desorption efficiency	Reference
<b>gCON</b>		<b>398</b> <b>(pH = 7.0)</b>	<b>20 min (1 g/L)</b>	<b>~97% (0.5 M NaOH)</b>	<b>This work</b>
MOF	UiO-66	85	2 h (1 g/L)	0.01 M NaOH	14
	UiO-66-NH <sub>2</sub>	92	2 h (1 g/L)	0.01 M NaOH	14
	UiO-66	135.4 (pH = 7.0)	1h (0.5 g/L)	NA	15
	Zr-loaded MIL-101	20.83 (pH = 6.5)	6 h (0.8 g/L)	0.003 M NaOH	16

Other porous materials					
	Compound	Adsorption capacity (mg/g)	Equilibrium time	phosphate desorption efficiency	Reference
Carbon-based	Zirconium-crosslinked graphene oxide/alginate	255.35	7 h (0.2 g/L)	NA	17
	ZrO <sub>2</sub> -functionalized graphite oxide	16.45 (pH = 6.0)	436 min (0.5 g/L)	95 % (0.1 M NaOH)	18
	Zirconium loaded reduced graphene oxide	27.71 (pH = 5.0)	375 min (0.2 g/L)	NA	19
Natural mineral based	Zirconium-modified zeolite	10.2 (pH = 7.0)	24 h (0.25 g/L)	NA	20
	Zr/Al-pillared montmorillonite	17.2 (pH = 5.0)	6 h (2 g/L)	NA	21
Membrane-based	ZrO <sub>2</sub> -embedded SiO <sub>2</sub> nanofibrous membrane	57.58 (pH = 7.0)	1 h (0.2 g/L)	95 % (0.1 M NaOH)	22
	Zr/PVA-modified PVDF membrane	21.64 (pH = 7.0)	30 h (0.5 g/L)	NA	23
Biomass-based	Zr-loaded orange waste gel	57 (pH = 7.0)	15 h (1.66 g/L)	95 % (0.2 M NaOH)	24
	Zr-loaded wheat straw	31.9	10 h (0.05 g/L)	98.2 % (5 wt % NaOH + 5 wt % NaCl)	25

	ZrO <sub>2</sub> -loaded amine crosslinked shaddock Peel	59.89 (pH = 3.0)	4 h (1 g/L)	NA	26
	Amino-functionalised magnetic zirconium alginate	58.73 (pH = 2.0)	30 h (2.5 g/L)	98.4 % (0.2 M NaOH)	27
	Zr-modified activated sludge	27.55 (pH = 4.0)	4.5 h (10 g/L)	NA	28
	ZrO <sub>2</sub> -loaded lignocellulosic butanol residue	7.17 (pH = 6.0)	250 min (0.625 g/L)	NA	29
Magnetic-based	Fe <sub>3</sub> O <sub>4</sub> @SiO <sub>2</sub> @ZrO <sub>2</sub>	39.1	5 h (3 g/L)	87 % (0.1 M KOH)	30
	Fe <sub>3</sub> O <sub>4</sub> @ZrO <sub>2</sub>	69.44 (pH = 5.0)	16 h (2.5 g/L)	88 % (1 M NaOH)	31
	ZrO <sub>2</sub> @SiO <sub>2</sub> @Fe <sub>3</sub> O <sub>4</sub>	6.33 (pH = 7.0)	60 min (0.5 g/L)	79 % (0.1 M NaOH + 1 M Na <sub>2</sub> SO <sub>4</sub> )	32
	ZrO <sub>2</sub> @Fe <sub>3</sub> O <sub>4</sub>	15.98 (pH = 7.0)	15 min (0.5 g/L)	88.2 % (1 M NaOH)	32
Polymer based	Zr-loaded collagen fiber	33.8 (pH = 6.0)	3 h (1 g/L)	NA	33
	Zirconium sulfate-loaded polymer	110 (pH = 7.0)	2 h (1 g/L)	NA	34
	ZrO <sub>2</sub> -loaded D-201	47.9 (pH = 6.5)	6 h (0.5 g/L)	~90 % (5 % NaOH + 5 % NaCl)	35
	ZrO <sub>2</sub> -loaded IRA-400	91.74	NA (0.8 g/L)	NA	36
	Zirconium molybdate-loaded anion exchange	42.2 (pH = 5.5)	9 h (0.5 g/L)	92 % (0.1 M NaOH)	37
	Zr(IV)-modified chitosan	47.44 (pH = 7.0)	20 min (2 g/L)	NA	38
	ZrO <sub>2</sub> -loaded PANI	32.4 (pH = 6.9)	24 h (1.3 g/L)	NA	39
	Zr-loaded magnetic IPN hydrogel	50.76 (pH = 6.5)	20 h (0.25 g/L)	96 % (0.05 M NaOH)	40
Molecularly imprinted polymer-based	GO-IIP	104.3	40 min (0.4 g/L)	91.05 % (0.02 M NaOH)	41
	MIP	78.88	60 min (0.5 g/L)	NA	42

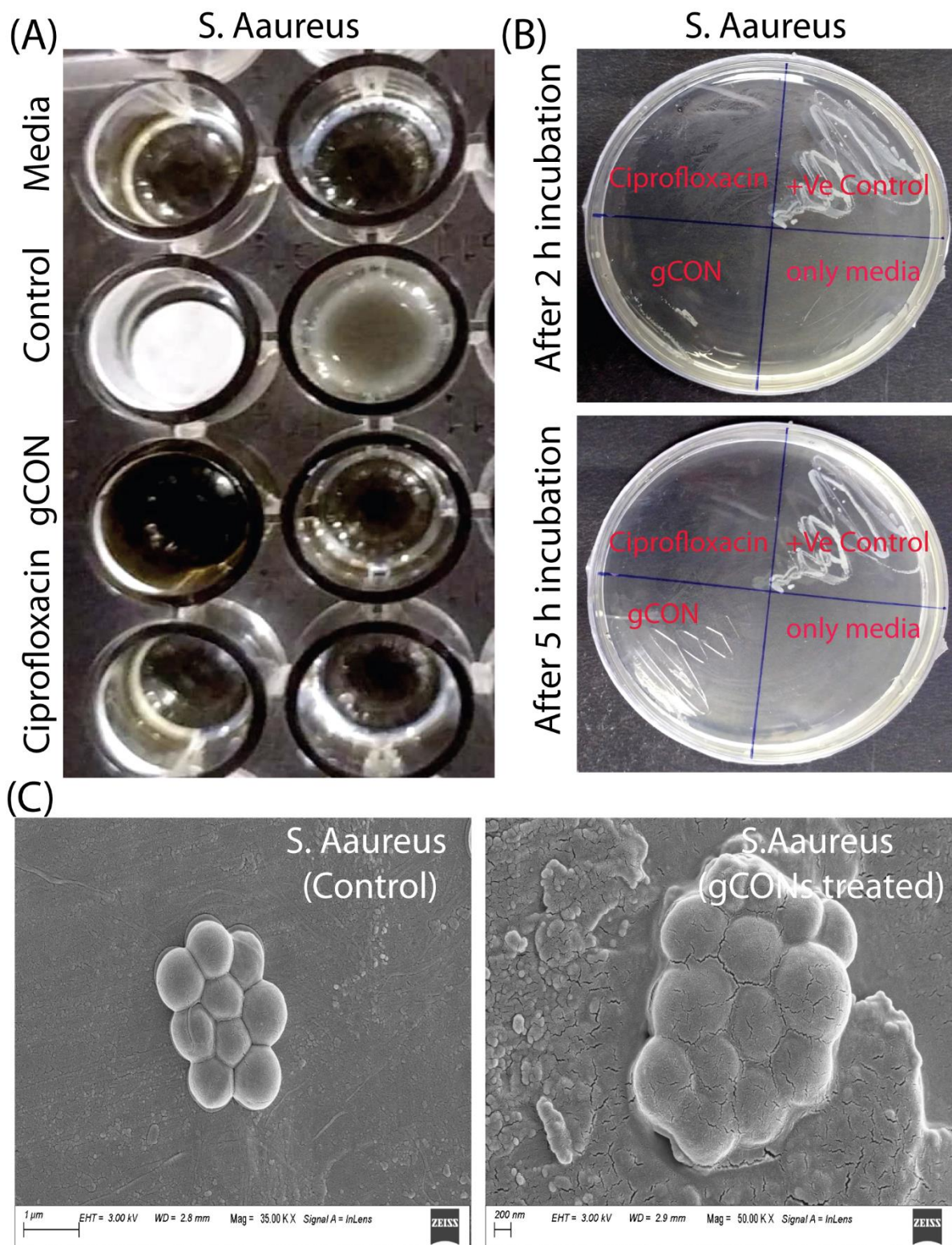
	ZnAl layered double hydroxide(ZnAl-LDH)	57.05	4 h (1 g/L)	~70 % (0.1 M NaOH)	43	
	MCM-41	45.16	10 min (1 g/L)	NA	44	
	SBA-15	mono-amino	33.17	10 min (1 g/L)	NA	45
		di-amino	52.7	10 min (1 g/L)	NA	45
		Tri-amino	76.26	10 min (1 g/L)	NA	45
		Mono-amino	69.97	15 min (1 g/L)	NA	46

NA = Not Available.

## 5. Antibacterial activities of the polymer:

**5.1. Antimicrobial studies** — Antimicrobial study of the polymer was performed against gram-negative representative bacteria (*Escherichia coli*, MTCC 1687) and gram-positive bacteria *Staphylococcus aureus* and its drug-resistant strain (MRSA) grown in Luria Bertani (LB) and Brain Heart Infusion (BHI), respectively. Bacterial cells were cultured in broth followed by streaking on the agar plates. During the antimicrobial study, the bacterial colony was inoculated in its respective broth media till its mid-logarithmic phase and harvested by centrifugation and suspended in media. In a microtiter, well plate gCON was stabilized, and on this layer, bacterial cells at  $10^6$  CFU/mL were added. For the control experiment, the sterile moist filter paper was taken. After 4 to 5 hr of incubation at  $37^\circ\text{C}$  10  $\mu\text{L}$  of the media was transferred to another new well (containing growth media) followed by plate incubation at  $37^\circ\text{C}$  for 16 to 20 hr. Bacterial growth was monitored by optical density measurement at 600 nm, or visibility of transparency of the wells as wells with bacterial growth was cloudy. Further to confirm the bactericidal activity of the polymer, this experiment was repeated, and 10  $\mu\text{L}$  from both the well were streaked onto the agar plate at two different time intervals.<sup>47</sup>

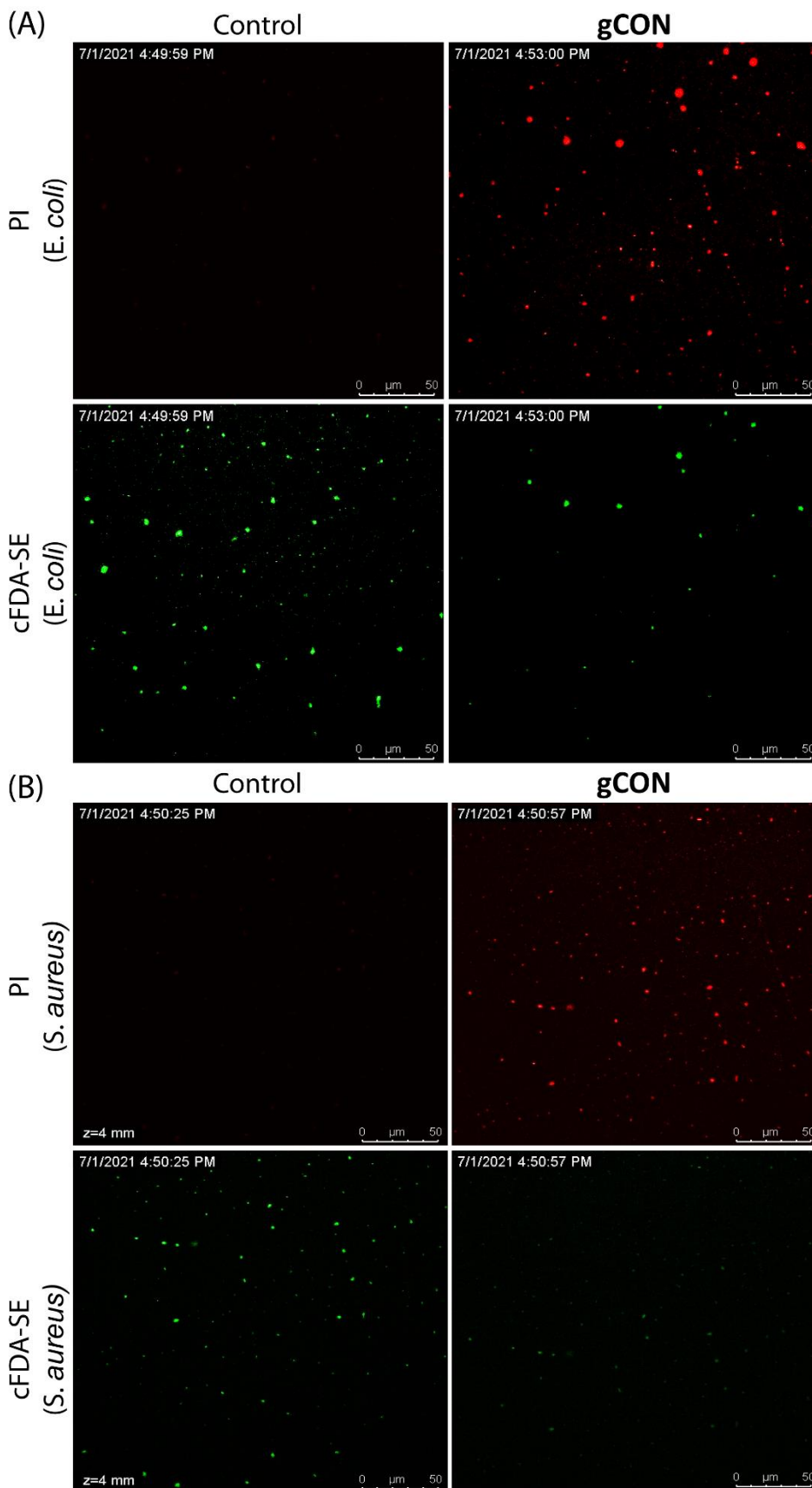
**5.2. Bacterial cell morphology by FESEM** — Bacterial cell morphology of polymer treated *E. coli* and MRSA cell was done by FESEM analysis. Bacterial cells were cultured as aforementioned till the exponential phase in LB and BHI and washed with phosphate buffer saline followed by Mili-Q water by centrifugation at 4000 rpm for 5 min. Cells were prepared by the drop-cast method on aluminium foil wrapped on a glass grid. Before analysis sample was stacked on a metal grid and gold-coated twice. The image was recorded by using the FESEM ZEISS Sigma-300 instrument.<sup>47</sup>



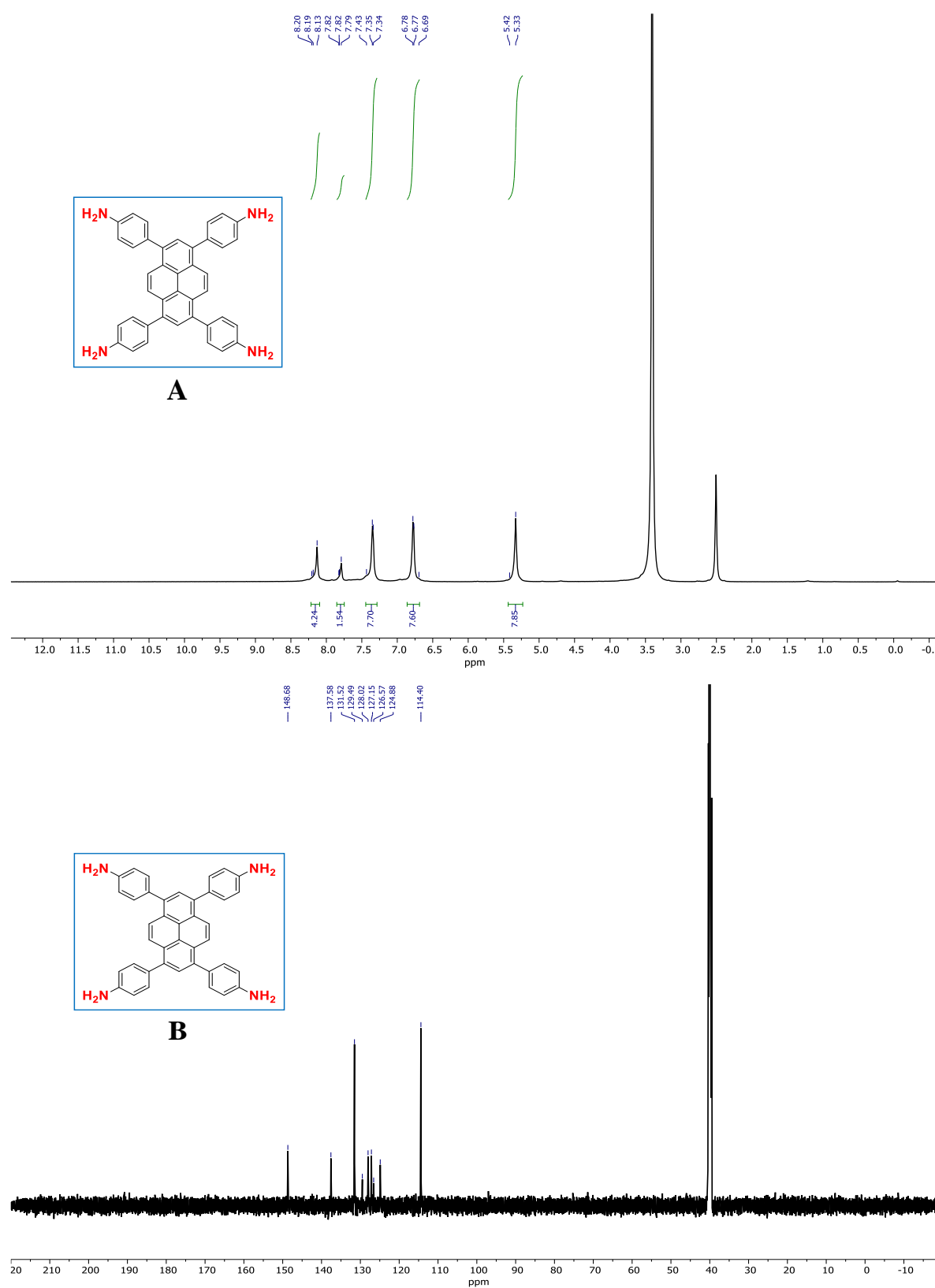
**Fig. S19.** Antibacterial activities of gCONs were investigated by the 96-well plate (A) and agar plate (B) method. FESEM images of control and gCONs treated *S. aureus* (C).

.....

**5.3. Live-dead fluorescence imaging of the bacterial cell** — Gram negative and Gram positive bacterial cells were cultured and harvested as in aforementioned antimicrobial study of the gCON.<sup>47, 48</sup> The gCON polymer treated bacterial cells were harvested and stained with propidium iodide (PI) and carboxyfluorescein diacetate succinimidyl ester (cFDA-SE). The PI dye can enter in membrane integrity compromised bacterial cells and intercalates between the DNA and shows the red fluorescence while cFDA-SE can enter in both live and dead cell but shows the green fluorescence only when an active esterase enzyme of the metabolically active bacterial cells degrades the ester group of the dye. Dye stained bacterial cells were mounted on to the glass slides and analyzed under the confocal microscope. (CLSM; Leica TCS SP8).



**Fig. S20.** Representative CLSM images of untreated and gCON treated *E. coli* (A) and *S. aureus* (B) cells. The scale bar for the images is 50  $\mu\text{m}$ .

5.  $^1\text{H}$  NMR and  $^{13}\text{C}$  NMR spectra of synthesized compounds:**Fig. S21.**  $^1\text{H}$  NMR (A) and  $^{13}\text{C}$  NMR (B) spectra of compound **2**.

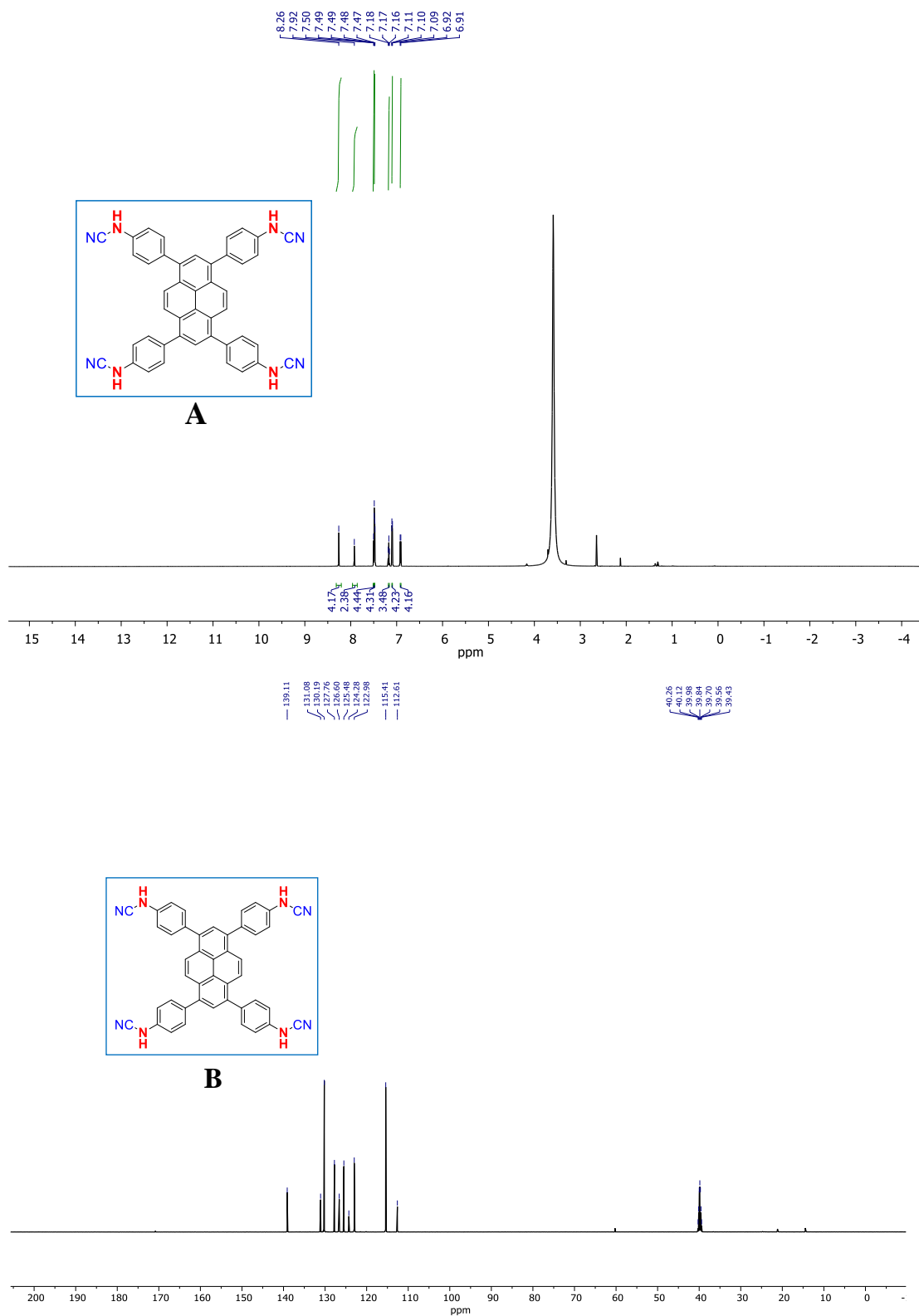


**Fig. S22.** <sup>1</sup>H NMR (A) and <sup>13</sup>C NMR (B) spectra of compound **3**.

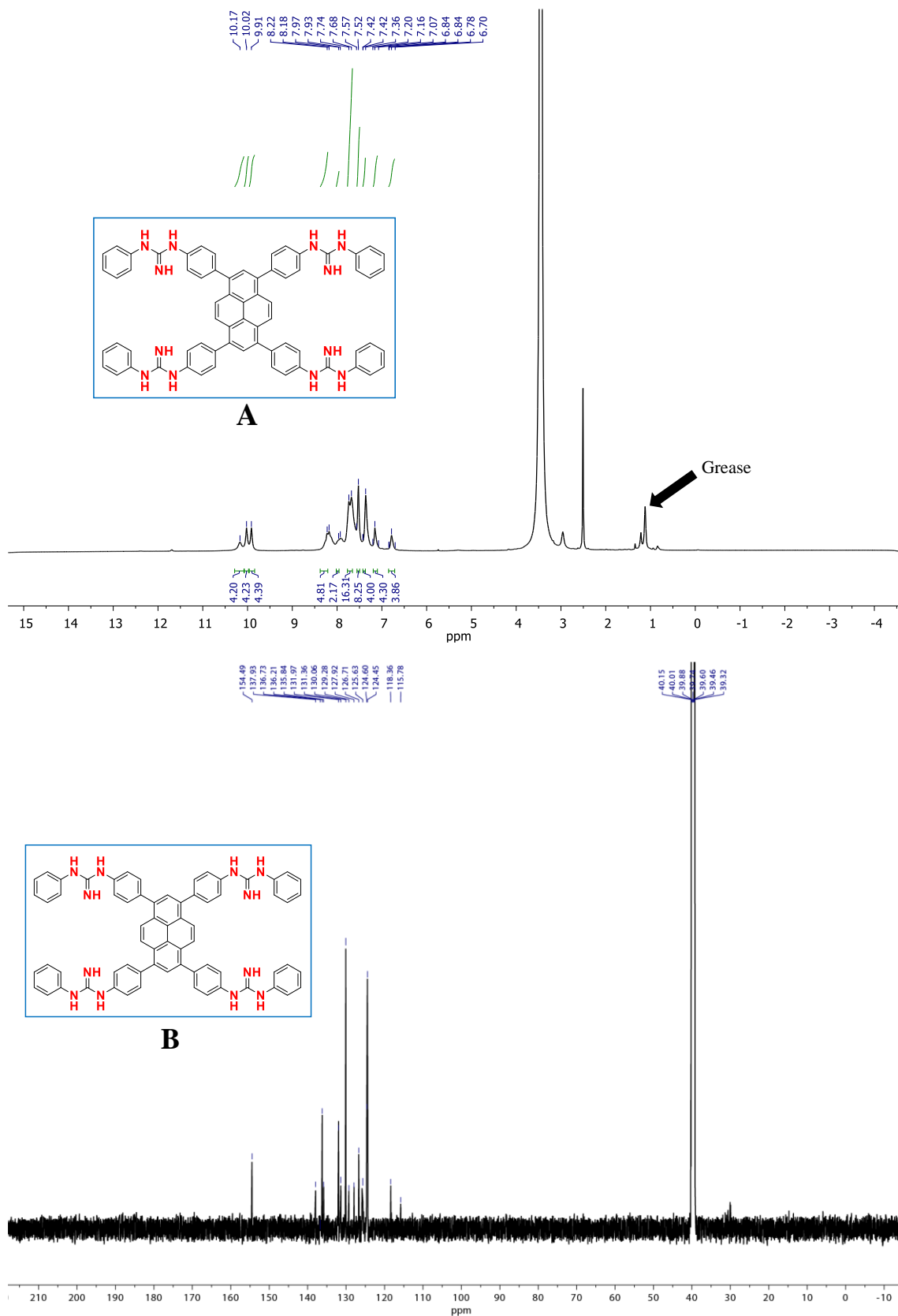
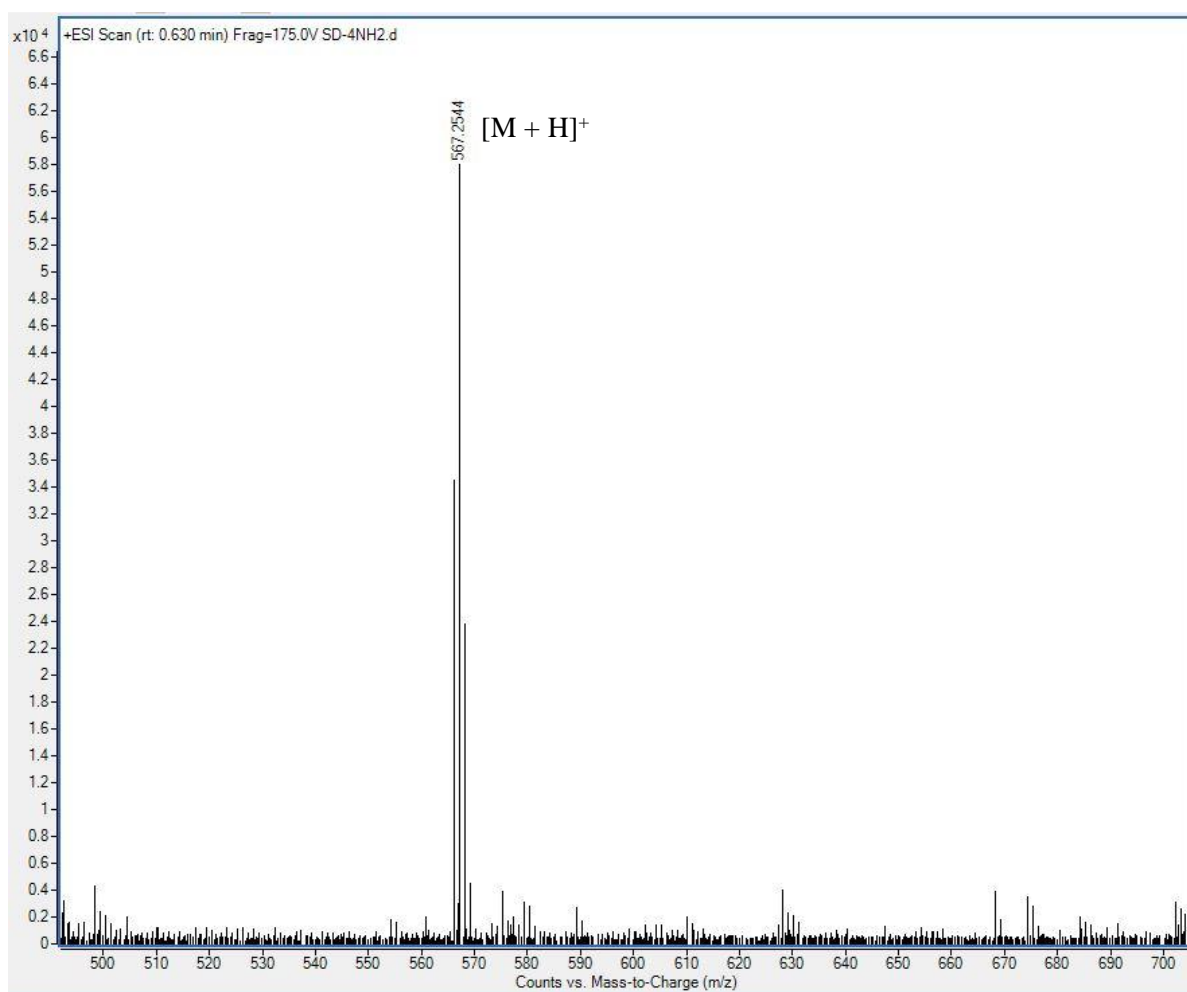
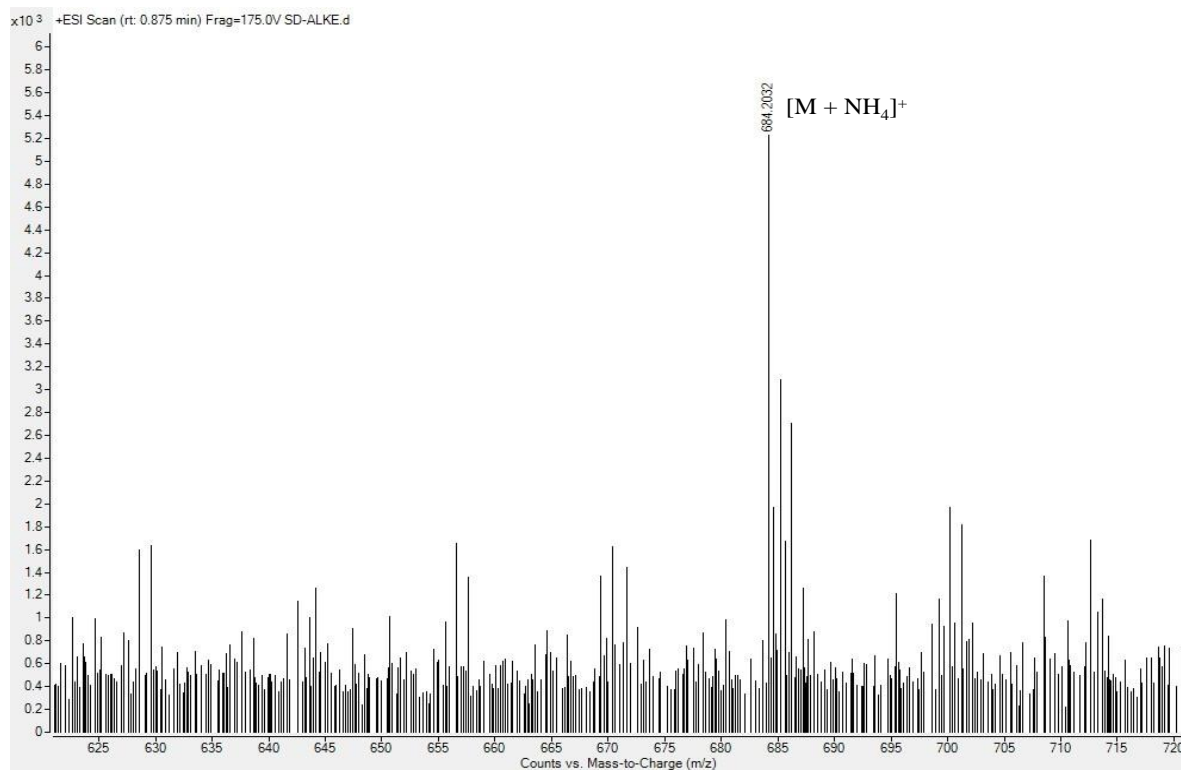
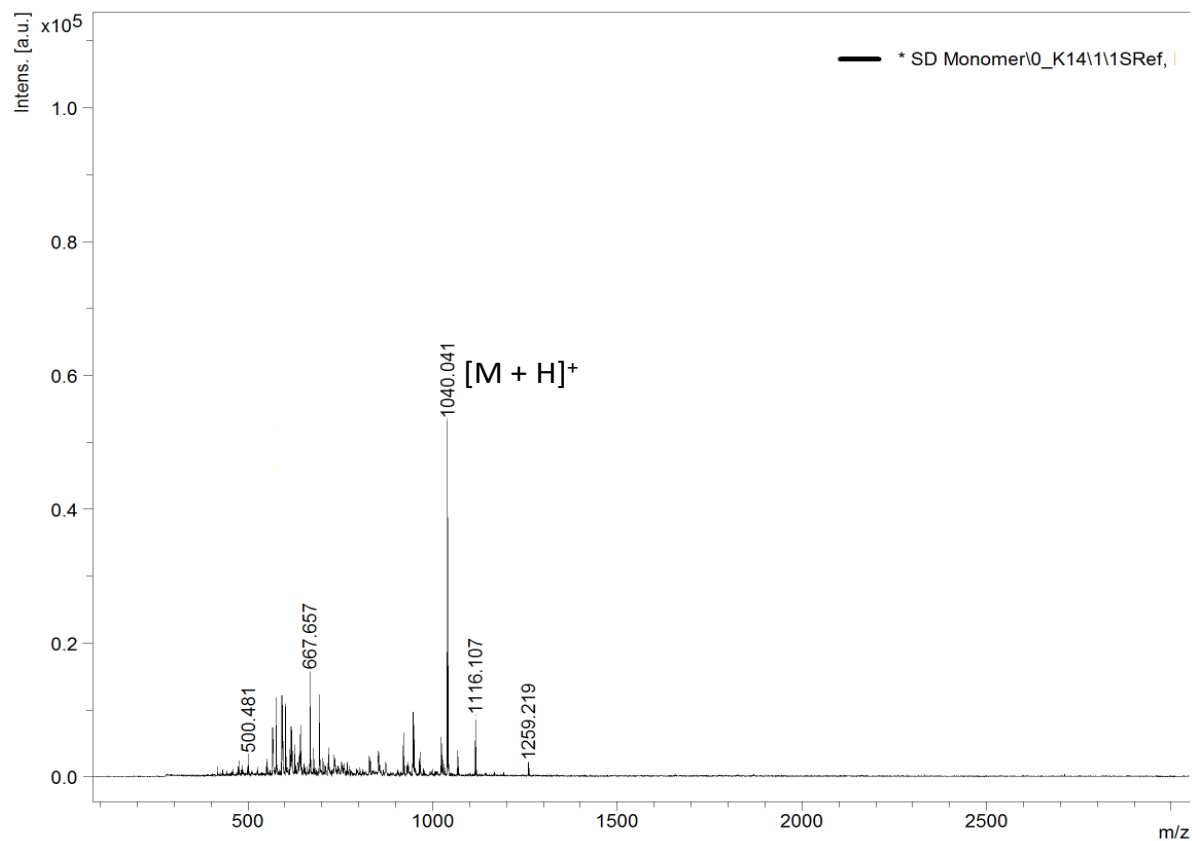


Fig. S23.  $^1\text{H}$  NMR (A) and  $^{13}\text{C}$  NMR (B) spectra of compound 4.

**6. Mass spectra of compounds:****Fig. S24.** HRMS spectra of compound **2**.



**Fig. S25.** ESI-MS spectra of compound **3**.



**Fig. S26.** MALDI spectra of compound **4**.

## 7. References:

1. K. C. Ranjeesh, R. Ilathvalappil, S. D. Veer, J. Peter, V. C. Wakchaure, Goudappagouda, K. V. Raj, S. Kurungot and S. S. Babu, *J. Am. Chem. Soc.*, 2019, **141**, 14950-14954.
2. F. Auras, L. Ascherl, A. H. Haldmioun, J. T. Margraf, F. C. Hanusch, S. Reuter, D. Bessinger, M. Doblinger, C. Hettstedt, K. Karaghiosoff, S. Herbert, P. Knochel, T. Clark and T. Bein, *J. Am. Chem. Soc.*, 2016, **138**, 16703-16710.
3. E. Mazzotta, S. Rella, A. Turco and C. Malitesta, *Rsc Adv.*, 2015, **5**, 83164-83186.
4. L. Paltrinieri, M. Wang, S. Sachdeva, N. A. M. Besseling, E. J. R. Sudholter and L. C. P. M. de Smet, *J. Mater. Chem. A*, 2017, **5**, 18476-18485.
5. J. P. Sylvestre, S. Poulin, A. V. Kabashin, E. Sacher, M. Meunier and J. H. T. Luong, *J. Phys. Chem. B*, 2004, **108**, 16864-16869.
6. TURBOMOLE V7.2 2017, a development of University of Karlsruhe and Forschungszentrum Karlsruhe GmbH, 1989-2007, *TURBOMOLE GmbH, since 2007*; available from <http://www.turbomole.com>.
7. J. P. Perdew, K. Burke and M. Ernzerhof, *Phys. Rev. Lett.*, 1996, **77**, 3865-3868.
8. S. Grimme, J. Antony, S. Ehrlich and H. Krieg, *J. Chem. Phys.*, 2010, **132**, 154104-154122.
9. A. Schäfer, C. Huber and R. Ahlrichs, *J. Chem. Phys.*, 1994, **100**, 5829-5835.
10. K. Eichkorn, O. Treutler, H. Öhm, M. Häser and R. Ahlrichs, *Phys. Lett.*, 1995, **240**, 283-289.
11. M. H. Sierka, A.; Ahlrichs, R., *J. Chem. Phys.*, 2003, **118**, 9136-9148.
12. A. Klamt and G. Schüürmann, *J. Chem. Soc., Perkin Trans.*, 1993, 799-805.
13. H. Asiabi, Y. Yamini and M. Shamsayei, *Chem. Eng. J.*, 2018, **337**, 609-615.
14. T. Guan, X. D. Li, W. K. Fang and D. Y. Wu, *Appl. Surf. Sci.*, 2020, **501**.
15. Y. Gu, D. Xie, Y. Ma, W. Qin, H. Zhang, G. Wang, Y. Zhang and H. Zhao, *ACS Appl. Mater. Interf.*, 2017, **9**, 32151-32160.
16. T. Liu, J. Feng, Y. Wan, S. Zheng and L. Yang, *Chemosphere*, 2018, **210**, 907-916.
17. S. J. Shan, H. Tang, Y. Zhao, W. Wang and F. Y. Cui, *Chem. Eng. J.*, 2019, **359**, 779-789.
18. E. M. Zong, D. Wei, H. Q. Wan, S. R. Zheng, Z. Y. Xu and D. Q. Zhu, *Chem. Eng. J.*, 2013, **221**, 193-203.
19. X. Luo, X. R. Wang, S. P. Bao, X. W. Liu, W. C. Zhang and T. Fang, *Sci. Rep.*, 2016, **6**.
20. M. J. Yang, J. W. Lin, Y. H. Zhan, Z. L. Zhu and H. H. Zhang, *Environ. Sci. Pollut. R.*, 2015, **22**, 3606-3619.
21. W. Y. Huang, J. Chen, F. He, J. P. Tang, D. Li, Y. Zhu and Y. M. Zhang, *Appl. Clay Sci.*, 2015, **104**, 252-260.
22. X. Q. Wang, L. Doug, Z. L. Li, L. Yang, J. Y. Yu and B. Ding, *Acs Appl. Mater. Inter.*, 2016, **8**, 34668-34676.
23. D. D. Zhao and J. P. Chen, *Ind. Eng. Chem. Res.*, 2016, **55**, 6835-6844.
24. B. K. Biswas, K. Inoue, K. N. Ghimire, H. Harada, K. Ohto and H. Kawakita, *Bioresource Technol.*, 2008, **99**, 8685-8690.
25. H. Qiu, C. Liang, X. L. Zhang, M. D. Chen, Y. X. Zhao, T. Tao, Z. W. Xu and G. Liu, *Acs Appl. Mater. Inter.*, 2015, **7**, 20835-20844.
26. P. J. Duan, X. Xu, Y. N. Shang, B. Y. Gao and F. F. Li, *J. Taiwan Inst. Chem. E*, 2017, **80**, 650-662.
27. H. Y. Luo, H. W. Rong, T. C. Zhang, X. Y. Zeng and J. Wan, *J. Appl. Polym. Sci.*, 2019, **136**.
28. J. H. Wang, X. H. Tong and S. Wang, *Water Air Soil Poll.*, 2018, **229**.

29. E. M. Zong, X. H. Liu, J. H. Jiang, S. Y. Fu and F. X. Chu, *Appl. Surf. Sci.*, 2016, **387**, 419-430.
30. A. Sarkar, S. K. Biswas and P. Pramanik, *J. Mater. Chem.*, 2010, **20**, 4417-4424.
31. Z. Wang, M. C. Xing, W. K. Fang and D. Y. Wu, *Appl. Surf. Sci.*, 2016, **366**, 67-77.
32. L. P. Fang, B. L. Wu and I. M. C. Lo, *Chem. Eng. J.*, 2017, **319**, 258-267.
33. X. P. Liao, Y. Ding, B. Wang and B. Shi, *Ind. Eng. Chem. Res.*, 2006, **45**, 3896-3901.
34. N. Pitakteeratham, A. Hafuka, H. Satoh and Y. Watanabe, *Water Res.*, 2013, **47**, 3583-3590.
35. L. Chen, X. Zhao, B. C. Pan, W. X. Zhang, M. Hua, L. Lv and W. M. Zhang, *J. Hazard Mater.*, 2015, **284**, 35-42.
36. N. Y. Acelas, B. D. Martin, D. Lopez and B. Jefferson, *Chemosphere*, 2015, **119**, 1353-1360.
37. T. H. Bui, S. P. Hong and J. Yoon, *Water Res.*, 2018, **134**, 22-31.
38. Q. Liu, P. Hu, J. Wang, L. J. Zhang and R. H. Huang, *J. Taiwan. Inst. Chem. E*, 2016, **59**, 311-319.
39. F. C. P. Masim, C. H. Tsai, Y. F. Lin, M. L. Fu, M. H. Liu, F. Kang and Y. F. Wang, *Environ. Technol.*, 2019, **40**, 226-238.
40. J. Wan, C. Zhu, J. Hu, T. C. Zhang, D. Richter-Egger, X. N. Feng, A. J. Zhou and T. Tao, *Appl. Surf. Sci.*, 2017, **423**, 484-491.
41. Z. C. Liu, W. Wu, Y. Liu and X. Hu, *J. Taiwan Inst. Chem. E*, 2018, **85**, 282-290.
42. Y. Xu, M. H. Huang and X. B. Luo, *Appl. Surf. Sci.*, 2019, **467**, 135-142.
43. Q. Q. Yu, Y. Q. Zheng, Y. P. Wang, L. Shen, H. T. Wang, Y. M. Zheng, N. He and Q. B. Li, *Chem. Eng. J.*, 2015, **260**, 809-817.
44. J. W. Choi, S. Y. Lee, S. G. Chung, S. W. Hong, D. J. Kim and S. H. Lee, *Water Air Soil Poll.*, 2011, **222**, 243-254.
45. S. Hamoudi, A. El-Nemr and K. Belkacemi, *J. Colloid. Interf. Sci.*, 2010, **343**, 615-621.
46. J. W. Choi, S. Y. Lee, S. H. Lee, K. B. Lee, D. J. Kim and S. W. Hong, *Water Air Soil Poll.*, 2012, **223**, 2551-2562.
47. A. Patel, S. Dey, K. Shokeen, T. M. Karpinski, S. Sivaprakasam, S. Kumar and D. Manna, *Rsc Med. Chem.*, 2021.
48. M. Yasir, D. Dutta and M. D. P. Willcox, *Sci. Rep.*, 2019, **9**, 7063.